Development/Plasticity/Repair

Neurog1 and *Neurog2* Control Two Waves of Neuronal Differentiation in the Piriform Cortex

Rajiv Dixit,[1]* Grey Wilkinson,[1]* Gonzalo I. Cancino,[3] Tarek Shaker,[1] Lata Adnani,[1] Saiqun Li,[1] Daniel Dennis,[1] Deborah Kurrasch,[1] Jennifer A. Chan,[2] Eric C. Olson,[4] David R. Kaplan,[3,5] Céline Zimmer,[6] and Carol Schuurmans[1]

[1]Departments of Biochemistry and Molecular Biology and Medical Genetics, Hotchkiss Brain Institute and Alberta Children's Hospital Research Institute, [2]Department of Pathology and Laboratory Medicine, Southern Alberta Cancer Research Institute, University of Calgary, Alberta T2N 4N1, Canada, [3]Programs in Cell Biology, and Developmental and Stem Cell Biology, Hospital for Sick Children, Toronto M5G 1L7, Canada, [4]Department of Neuroscience and Physiology, SUNY Upstate Medical University, Syracuse, New York 13210, [5]Institute of Medical Science and Department of Molecular Genetics, University of Toronto, Toronto M5S 1A8, Canada, and [6]Division of Molecular Neurobiology, National Institute for Medical Research, Mill Hill, London NW7 1AA, United Kingdom

The three-layered piriform cortex, an integral part of the olfactory system, processes odor information relayed by olfactory bulb mitral cells. Specifically, mitral cell axons form the lateral olfactory tract (LOT) by targeting lateral olfactory tract (lot) guidepost cells in the piriform cortex. While lot cells and other piriform cortical neurons share a pallial origin, the factors that specify their precise phenotypes are poorly understood. Here we show that in mouse, the proneural genes *Neurog1* and *Neurog2* are coexpressed in the ventral pallium, a progenitor pool that first gives rise to Cajal-Retzius (CR) cells, which populate layer I of all cortical domains, and later to layer II/III neurons of the piriform cortex. Using loss-of-function and gain-of-function approaches, we find that *Neurog1* has a unique early role in reducing CR cell neurogenesis by tempering *Neurog2*'s proneural activity. In addition, *Neurog1* and *Neurog2* have redundant functions in the ventral pallium, acting in two phases to first specify a CR cell fate and later to specify layer II/III piriform cortex neuronal identities. In the early phase, *Neurog1* and *Neurog2* are also required for lot cell differentiation, which we reveal are a subset of CR neurons, the loss of which prevents mitral cell axon innervation and LOT formation. Consequently, mutation of *Trp73*, a CR-specific cortical gene, results in lot cell and LOT axon displacement. *Neurog1* and *Neurog2* thus have unique and redundant functions in the piriform cortex, controlling the timing of differentiation of early-born CR/lot cells and specifying the identities of later-born layer II/III neurons.

Key words: **Cajal-Retzius neurons; lateral olfactory tract guidepost cells; *Neurog1* and *Neurog2*; piriform cortex; proneural genes; ventral pallium**

Introduction

The cerebral cortex, which includes the archicortex, neocortex, and piriform cortex, is derived from the dorsal telencephalon, or pallium. Based on gene expression, the pallium is subdivided into medial, dorsal, lateral, and ventral domains, each giving rise to distinct cortical territories (Puelles et al., 2000; Yun et al., 2001). Cajal-Retzius (CR) cells are an early-born cortical lineage, differentiating between embryonic day (E) 10.5 and E12.5 in mouse (Smart and Smart, 1977; Wood et al., 1992; Marin-Padilla, 1998; Supèr et al., 1998). CR cells arise from three sites in the pallial margins: (1) medially, the cortical hem/choroid plexus; (2) rostrally, the pallial septum/rostrobulbar area; and (3) laterally, the ventral pallium (Takiguchi-Hayashi et al., 2004; Bielle et al., 2005; Yoshida et al., 2006; Zhao et al., 2006; García-Moreno et al., 2007; Imayoshi et al., 2008). Given their pallial origins, most CR cells are labeled in an *Emx1*-lineage trace (Gorski et al., 2002) and express Tbr1 (Hevner et al., 2003), both cortical-specific transcription factors. Many CR cells also express Reelin (Alcántara et al., 1998), a secreted glycoprotein that guides radial migration of neocortical neurons (Caviness, 1982; Howell et al., 1997).

While neocortical development has been well studied, much less is known about the three-layered piriform cortex. The piriform cortex is a central component of the olfactory system, which together with the olfactory epithelium (OE) and olfactory bulb (OB) is responsible for detecting and processing odors. Superficial layer II and deep layer III of the piriform cortex contain glutamatergic projection neurons and interspersed GABAergic interneurons (Sarma et al., 2011), while layer I is a cell-sparse zone containing CR neurons and lateral olfactory tract (lot) guidepost cells. Lot cells guide innervation of the anterior piri-

Received Feb. 8, 2013; revised Nov. 17, 2013; accepted Nov. 20, 2013.

Author contributions: R.D., D.K., C.Z., and C.S. designed research; R.D., G.W., G.I.C., T.S., L.A., S.L., D.D., and C.Z. performed research; G.I.C., D.K., J.C., E.C.O., and D.R.K. contributed unpublished reagents/analytic tools; R.D., G.W., C.Z., and C.S. analyzed data; R.D., C.Z., and C.S. wrote the paper.

This work was supported by a Canadian Institutes of Health Research (CIHR; MOP-44094) Operating Grant to C.S., C.S. is an Alberta Innovates Health Solutions Senior Scholar. R.D. was supported by a CIHR Canada Hope Scholarship and G.W. and S.L. were supported by a CIHR Training Grant in Genetics, Child Development and Health. We thank François Guillemot, David Anderson, Tak Mak, Tatsumi Hirata, Daniel Dufort, Masato Nakafuku, and Valerie Wallace for generously providing reagents or mice. We also thank Nicole Gruenig, Dawn Zinyk, Pierre Mattar, and Natasha Klenin for technical support.

The authors declare no competing financial interests.

*R.D. and G.W. contributed equally to this work.

Correspondence should be addressed to Carol Schuurmans at the above address. E-mail: cschuurm@ucalgary.ca.

DOI:10.1523/JNEUROSCI.0614-13.2014

 0270-6474/14/340539-15$15.00/0

form cortex by OB mitral cells, the axons of which form the LOT (note that lot guidepost cells are distinguished from LOT axons by small and capital letters, respectively; Sato et al., 1998). We noted several striking similarities between lot cells (Sato et al., 1998; Tomioka et al., 2000) and CR neurons (Wood et al., 1992; Hevner et al., 2003; Takiguchi-Hayashi et al., 2004): both act as cellular guideposts for axonal tract formation, have a pallial origin, are among the earliest born cortical neurons (lot cells also differentiate between E9.5 and E11), and migrate tangentially from their pallial sites of origin to populate the piriform cortex (Sato et al., 1998; Tomioka et al., 2000). However, while CR cell differentiation is well understood, the factors that specify a lot cell identity, and more globally control neuronal fate specification in the piriform cortex, remain poorly characterized.

Here we demonstrate that the proneural basic helix-loop-helix (bHLH) transcription factors *Neurog1* and *Neurog2,* which specify a neocortical projection neuron identity (Fode et al., 2000; Schuurmans et al., 2004), also specify piriform cortical neuronal identities. Specifically, *Neurog1* and *Neurog2* are required in two differentiation waves—first acting in opposition to control lot cell differentiation, which we reveal are a subpopulation of CR neurons, the localization of which depends on *Trp73*, and later controlling the differentiation of layer II/III piriform cortical neurons.

Materials and Methods

Animals and genotyping. Animal procedures followed guidelines of the Canadian Council of Animal Care and were approved by the University of Calgary Animal Care Committee (Protocol AC11-0053), the Institutional Animal Care and Use Committee of State University of New York Upstate Medical University, and the Hospital for Sick Children Animal Care Committee. Embryos of either sex were used throughout. *Neurog1* (Ma et al., 1998) and *Neurog2*$^{GFP\,KI}$ (Britz et al., 2006) mutant alleles were maintained on a CD1 background (Charles River) and genotyped as described (Ma et al., 1998; Britz et al., 2006). *Lef/Tcf-lacZ* transgenics were provided by Valerie Wallace and Daniel Dufort (Mohamed et al., 2004) and genotyped using forward (CCATCCAGAGACAAGCGAAGAC) and reverse (TTGAGGGGACGACGACAGT ATC) primers (35 cycles of 95°C/1′, 58°C/1′, 72°C/1.5′, then final extension 72°C/10′). *TAp73* mutants were genotyped using the following primers: *TAp73*WT: CTGGTCCAGGAGGTGAGACTGAGGC; *TAp73* Common: CTGGCCCTCTCAGCTTGTGCCACTTC, and *TAp73Neo*: GTGGGGGTGGGATTAGATAAATGCCTG (*TAp73*WT and *TAp73* Common for wild-type allele, 1 kb; and *TAp73Neo* and *TAp73* Common for mutant allele, 1.2 kb; 35 cycles of 94°C/45 s, 65°C/30 s, 72°C/1.5 min). *Trp73* (*p73*) mutants were genotyped using three primer PCRs: *p73*-1: GGGCCATGCCTGTCTACAAGAA; *p73*-2: CCTTCTACACGGATGAGGTG; *p73*-3:GAAAGCGAAGGAGCAAAGCTG (wild type, 550 bp; mutant, 400 bp; 40 cycles of 94°C/30 s, 64°C/30 s, 72°C/40 s). *Reeler* mutants (B6C3Fe a/a-*Relnrl*/+) were obtained from Jackson Laboratories and genotyped as described previously (D'Arcangelo et al., 1996).

Tissue processing, histology, and β-galactosidase histochemical staining. For histology, whole E18.5 heads were fixed in Bouin's solution, embedded in paraffin, and cut into 7 μm sections, which were stained with hematoxylin and eosin as previously described (Fode et al., 1998). For all other tissue studies, embryos were fixed overnight in 4% paraformaldehyde (PFA) in 1× PBS, pH 7.4, at 4°C, washed in 1× PBS, and cryoprotected in 20% sucrose in 1× PBS overnight at 4°C before embedding and freezing in Tissue Tek OCT (Sakura Finetek). Ten-micrometer cryosections were collected on Superfrost plus slides (Fisher Scientific). X-gal histochemical staining was performed on cryostat sections as follows. Sections were first washed 3 × 10 min in lacZ wash buffer (2 mM $MgCl_2$/0.01% sodium deoxycholate/0.02% Nonidet-P40/100 mM sodium phosphate, pH 7.3) before staining overnight at 37°C in wash buffer containing 5 mM potassium ferrocyanide, 5 mM potassium ferricyanide, and 0.67 mg/ml X-gal (Invitrogen). Slides were then washed in PBS, rinsed in water, and allowed to dry before mounting in Permount (Fisher Scientific).

RNA in situ *hybridization.* RNA *in situ* hybridization was performed as previously described (Alam et al., 2005) using digoxygenin-labeled riboprobes that were generated using a 10× labeling mix according to the manufacturer's instructions (Roche Diagnostics). Riboprobes were generated from linearized plasmid templates as follows: *Reln* (EcoRI/T3), *Trp73* (SalI/T3), *Etv1* (SpeI/T7), *Ctip2* (IMAGE 4457123; SalI/T7), *Id2* (HindIII/T3), *Dlx1* (XbaI/T3), *Wnt7b* (NcoI/SP6), *mGluR1* (IMAGE 30536724; EcoRI/T3), and *Dbx1* (IMAGE 5718470; EcoRI/T3).

Immunostaining and imaging. Immunostaining was performed on 10 μm cryostat sections that were processed and collected as described above. Cryosections were blocked either in 10% normal goat or donkey serum in 0.1% Triton X-100 in 1 × PBS or in 1 × Tris-buffered saline (25 mM Tris-HCl, pH 7.4, 0.14 M NaCl). Primary antibodies included: rabbit anti-calretinin (1:500; Swant), mouse anti-Ascl1 (1:200; BD Biosciences), mouse anti-Neurog2 (1:20; gift from David Anderson), rabbit anti-Neurog2 (1:500; gift from Masato Nakafuku), rabbit anti-Neurog1 (1:500; gift from Jane Johnson), rabbit anti-GFP (1:500; Millipore Bioscience Research Reagents), sheep anti-GFP (1:750; Biogenesis), rabbit anti-Tbr1 (1:3000, Millipore Bioscience Research Reagents), mouse anti-Reelin (1:500; Millipore Bioscience Research Reagents), rabbit anti-activated caspase 3 (1:100; Promega), mouse anti-MAP2 (1:500; Sigma-Aldrich), rabbit anti-Pax6 (1:500; Covance), rabbit-anti-Trp73 (1:500; Bethyl Laboratories), and rat anti-lot1 (1:200; gift from Tatsumi Hirata). Species-specific secondary antibodies were conjugated to Alexa488 (1:500; Invitrogen), Cy3 (1:500; Jackson Immunoresearch), or horseradish peroxidase (HRP). Sections were counterstained with DAPI (4,6-diamidino-2-phenylindole, 1:10,000; Sigma-Aldrich) and mounted in AquaPolymount (Polysciences). DAB staining of HRP-conjugated antibodies was performed using the Vectastain ABC kit according to the manufacturer's instructions (Vector Laboratories).

DiI tracing. E18.5 brains were fixed for 2 d in 4% PFA in 1× PBS at 4°C. Carbocyanin DiI crystals (Invitrogen) were introduced into the OB, and the brains were incubated at 37°C in 4% PFA in 1× PBS to allow dye diffusion for 2–3 weeks, followed by imaging.

In vitro *electroporation and quantitation.* The pCIG2-*Neurog2* expression vector was previously described (Mattar et al., 2008). The *Neurog1* cDNA was similarly PCR amplified and subcloned into pCIG2. *Ex vivo* electroporation and culture of E10.5 embryos were performed as previously described (Zimmer et al., 2010). Cell counts were performed on ≥3 independent embryos and on three sections per embryo. Error bars reflect SEM. Student's *t* tests were performed with *p* values denoted as follows: $^{*}p < 0.05$, $^{**}p < 0.01$, $^{***}p < 0.005$.

Results

Neurog1 and Neurog2 are coexpressed in ventral pallial progenitors and derivative lineages in both the neocortex and piriform cortex

Neocortical progenitors undergo temporal identity transitions (Pearson and Doe, 2004), first giving rise to CR neurons, then sequentially generating glutamatergic pyramidal neurons in neocortical layers VI, V, IV, and finally II/III (fused in mouse; Takahashi et al., 1999). *Neurog2* functions iteratively in this process, first promoting the differentiation of CR neurons (Imayoshi et al., 2008) and then functioning with *Neurog1*, a related proneural gene, to specify the glutamatergic identities of layer V/VI neurons (Fode et al., 2000; Schuurmans et al., 2004). Currently, it is not known whether *Neurog1* also functions in CR development, nor is it known whether *Neurog1* and *Neurog2* specify neuronal identities in the three-layered piriform cortex, which is an evolutionarily more ancient structure. We addressed these two questions herein.

The piriform cortex is derived from the ventral pallium (Puelles et al., 2000; Hirata et al., 2002), which also serves as one of three CR cell progenitor domains (in addition to the pallial septum and cortical hem; Fig. 1*A*). Thus, first asking whether *Neurog1* and *Neurog2* were expressed in ventral pallial progenitors, we examined cortices between E10.5 and E12.5, the period when CR cells (Wood et al., 1992; Hevner et al., 2003; Takiguchi-Hayashi et al., 2004) and layer

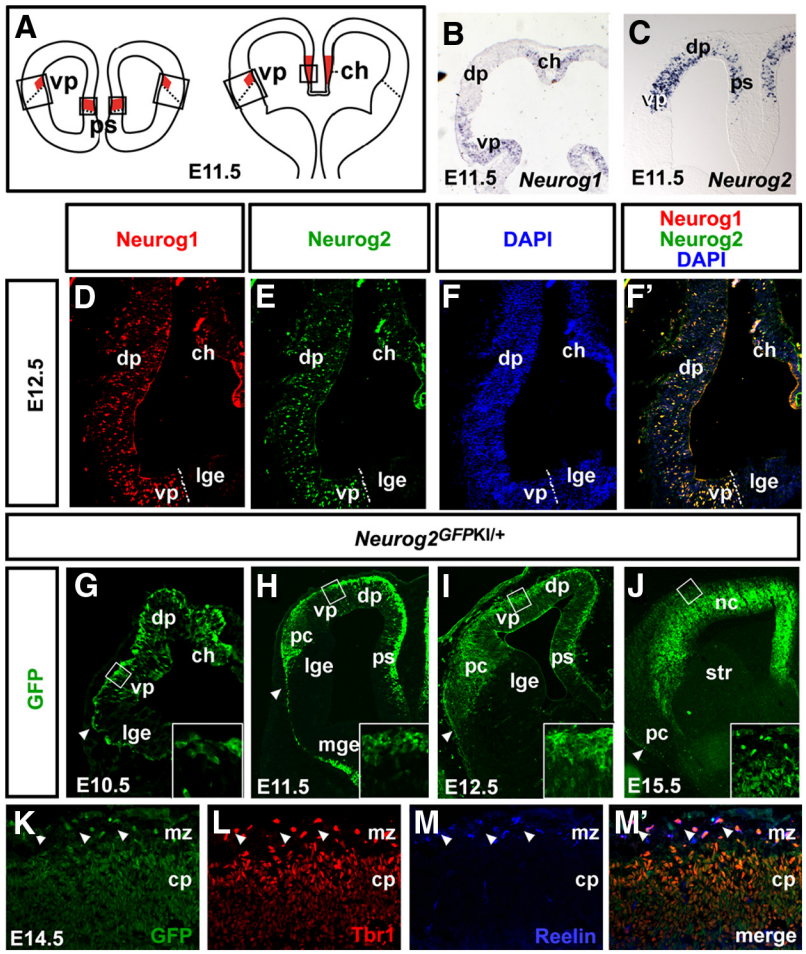

Figure 1. Neurog1 and Neurog2 are coexpressed in CR progenitors. ***A***, Schematic representation of the three main sites of CR cell production. ***B***, ***C***, Distribution of *Neurog1* (***B***) and *Neurog2* (***C***) transcripts in the E11.5 telencephalon. ***D–F***, ***F′***, Expression of Neurog1 (***D***, ***F′***, red), Neurog2 (***E***, ***F′***, green), and DAPI counterstain (***F***, ***F′***, blue) in E12.5 telencephalon. The dotted lines mark the pallial–subpallial border. ***G–J***, Expression of GFP in E10.5 (***G***), E11.5 (***H***), E12.5 (***I***), and E15.5 (***J***) *Neurog2*$^{GFP\,KI/+}$ cortices. Insets are high-magnification images of the boxed areas in the preplate (E10.5–E12.5) and marginal zone (E15.5). Arrowhead in mark the pallial-subpallial border. ***K–M***, ***M′***, Coexpression of GFP (***K***, ***M′***, green), Tbr1 (***L***, ***M′***, red), and Reelin (***M***, ***M′***) in E15.5 *Neurog2*$^{GFP\,KI/+}$ neocortex. Arrowheads mark CR neurons coexpressing all three markers in the marginal zone. ch, Cortical hem; cp, cortical plate; dp, dorsal pallium; lge, lateral ganglionic eminence; mge, medial ganglionic eminence; mz, marginal zone; nc, neocortex; ps, pallial septum; str, striatum; vp, ventral pallium.

III piriform cortex neurons arise (Hirata et al., 2002). At E10.5 (data not shown) and E11.5, *Neurog1* and *Neurog2* transcripts (Fig. 1*B*,*C*) and protein (data not shown) were detected in scattered pallial progenitors in a high-lateral to low-medial gradient, with elevated expression levels particularly evident in the ventral pallium, cortical hem, and pallial septum.

By E12.5, Neurog1 and Neurog2 were more broadly expressed in scattered progenitors throughout the pallial ventricular zone (VZ), including in the three sites of CR cell production (Fig. 1*D–F*′; data not shown). Quantification of proneural expression in E12.5 CR progenitor domains revealed that Neurog1 (ventral pallium; 11.3 ± 1.1% of DAPI$^+$ cells, $n = 3$, 1372 cells; cortical hem: 6.9 ± 0.2% of DAPI$^+$ cells; $n = 3$, 2980 cells) was expressed in fewer CR progenitors than Neurog2 (ventral pallium; 24.4 ± 6.1% of DAPI$^+$ cells, $n = 3$, 1372 cells; cortical hem: 11.6 ± 0.5% of DAPI$^+$ cells; $n = 3$, 2980 cells). Nevertheless, the vast majority of Neurog1$^+$ progenitors coexpressed Neurog2 (ventral pallium: 97.8 ± 1.5%, $n = 3$, 1372 cells; cortical hem: 89.1 ± 4.3%, $n = 3$, 2980 cells), indicating that these proneural genes are coexpressed in a common lineage.

Given that Neurog2$^+$ pallial progenitors largely encompass the Neurog1$^+$ population, we performed short-term lineage tracing in *Neurog2*$^{GFP\,KI/+}$ cortices to capture both lineages, taking advantage of GFP perdurance in derivative neurons. In E10.5–E15.5 *Neurog2*$^{GFP\,KI/+}$ cortices, GFP$^+$ cells were detected in the neocortical and piriform cortical marginal zones (Fig. 1*G–J*), where CR cells reside. GFP expression was also detected in the germinal zones and mantle layers of the neocortex and piriform cortex (Fig. 1*G–J*,*K*,*M*′). Within the E14.5 *Neurog2*$^{GFP\,KI/+}$ marginal zone, the vast majority of GFP$^+$ cells coexpressed Reelin, a CR cell marker (Alcántara et al., 1998), and Tbr1, a cortical-specific T-box protein (Hevner et al., 2003; Fig. 1*K–M*′). This is consistent with the pallial identity of CR neurons (Hevner et al., 2003) and with our previous short-term lineage-tracing experiments in E11.5 *Neurog2*$^{GFP\,KI/+}$ neocortices (Dixit et al., 2011b).

Thus, Neurog2$^+$ pallial progenitors, which largely encompass the Neurog1$^+$ pallial progenitor pool, give rise to CR cells that populate the marginal zones of both the piriform cortex and neocortex as well as the mantle zones of both structures.

Neurog2 single and *Neurog1* and *Neurog2* double mutants display early and spatially distinct deficiencies in CR cells

It was previously reported that fewer CR cells are generated in E12.5 and E14.5 *Neurog2*$^{-/-}$ neocortices (Imayoshi et al., 2008). However, this study did not address *Neurog2* function in CR cells in the piriform cortex, nor did it address whether *Neurog1* also contributes to CR cell development. We therefore compared CR cell numbers in *Neurog1* and *Neurog2* single mutants as well as *Neurog1* and *Neurog2* double mutants (hereafter *Neurog1/2*) at E12.5, when CR differentiation is mostly complete. We first analyzed the neocortical preplate for *Reln* expression. Compared with E12.5 wild-type neocortices (111.4 ± 7.0 *Reln*$^+$ cells/field; $n = 3$; Fig. 2*A*,*A*′,*M*), the number of *Reln*$^+$ cells was reduced to a similar extent (1.3-fold and 1.4-fold, respectively) in *Neurog2*$^{-/-}$ (88.6 ± 5.0 *Reln*$^+$ cells/field; $n = 3$; $p < 0.05$; Fig. 2*C*,*C*′,*M*) and *Neurog1*$^{-/-}$;*Neurog2*$^{-/-}$ (hereafter referred to as *Neurog1/2*$^{-/-}$) neocortices (75.4 ± 5.9 *Reln*$^+$ cells/field; $n = 2$; $p < 0.01$; Fig. 2*D*,*D*′,*M*). In contrast, 1.3-fold more *Reln*$^+$ cells were detected in the *Neurog1*$^{-/-}$ neocortical preplate (143.3 ± 6.0 *Reln*$^+$ cells/field; $n = 3$; $p < 0.01$; Fig. 2*B*,*B*′,*M*). Notably, the increase in *Reln*$^+$ CR cells in *Neurog1*$^{-/-}$ neocortices is consistent with our previous demonstration that E10.5–E12.5 *Neurog1*$^{-/-}$ neocortices undergo precocious neurogenesis, although these ectopic neurons were not previously identified as CR cells (Fode et al., 2000; Mattar et al., 2004). Strikingly, precocious neurogenesis is also observed in *Neurog1/2*$^{-/-}$ neocortices (Fode et al., 2000; Mattar et al., 2004), yet these neurons do not acquire a CR cell fate (Fig. 2*D*,*D*′,*M*). We

interpret these results in the following way. While either *Neurog1* or *Neurog2* can specify a CR cell identity, *Neurog1* has an added role, which is to slow down the rate of early cortical neurogenesis. Consistent with this interpretation, *Neurog2*$^{-/-}$ CR cell loss is restricted to dorsomedial domains (Fig. 2*C*), where *Neurog1* expression is lost (Fode et al., 2000), such that this region is equivalent to a *Neurog1/2* double mutant.

To further substantiate the roles of *Neurog1* and *Neurog2* in CR cell genesis, we also analyzed Tbr1 expression, which labels CR neurons as well as deep-layer cortical neurons (Hevner et al., 2003). In E12.5 embryos of all genotypes, Tbr1 was expressed in the neocortical and piriform cortical preplates, albeit at higher levels in *Neurog1*$^{-/-}$ cortices, which produce more CR neurons, and at lower levels in *Neurog2*$^{-/-}$ and *Neurog1/2*$^{-/-}$ cortices, where CR cell numbers are reduced (Fig. 2*E–H*'). In addition, Tbr1 was expressed in a wedge of cells adjacent to the lateral ganglionic eminence (LGE), demarcating the nascent piriform cortex, in all genotypes, except *Neurog1/2*$^{-/-}$ double mutants (Fig. 2*E–H*). Similar results were obtained when monitoring *Trp73* expression, which labels CR cells derived from the pallial septum and cortical hem (Meyer et al., 2002, 2004): 1.4-fold more *Trp73*$^{+}$ cells in the *Neurog1*$^{-/-}$ preplate (62.2 ± 3.6 *Trp73*$^{+}$ cells/field; $n = 3$; $p < 0.0001$; Fig. 2*J*,*J*',*N*) compared with wild type (44.5 ± 2.2 *Trp73*$^{+}$ cells/field; $n = 3$; Fig. 2*I*,*I*',*N*). Conversely, *Trp73*$^{+}$ cell numbers were reduced 1.9-fold and 2.7-fold in *Neurog2*$^{-/-}$ (23.2 ± 2.0 *Trp73*$^{+}$ cells/field; $n = 3$; $p < 0.0001$; Fig. 2*K*,*K*',*N*) and *Neurog1/2*$^{-/-}$ (16.6 ± 2.1 *Trp73*$^{+}$ cells/field; $n = 2$; $p < 0.0001$; Fig. 2*L*,*L*',*N*) neocortices, respectively. Moreover, in the nascent piriform cortex, where *Trp73*$^{+}$ cells normally accumulate in a lateral wedge, a striking loss of *Trp73*$^{+}$ CR cells was observed specifically within *Neurog1/2*$^{-/-}$ embryos (Fig. 2*L*).

Thus, CR cell differentiation in both the neocortex and piriform cortex requires either *Neurog1* or *Neurog2*. In addition, *Neurog1* has an additional role, which is to slow down the genesis of early-born cortical neurons, including CR cells, ensuring that appropriate numbers of these early-born neurons are generated.

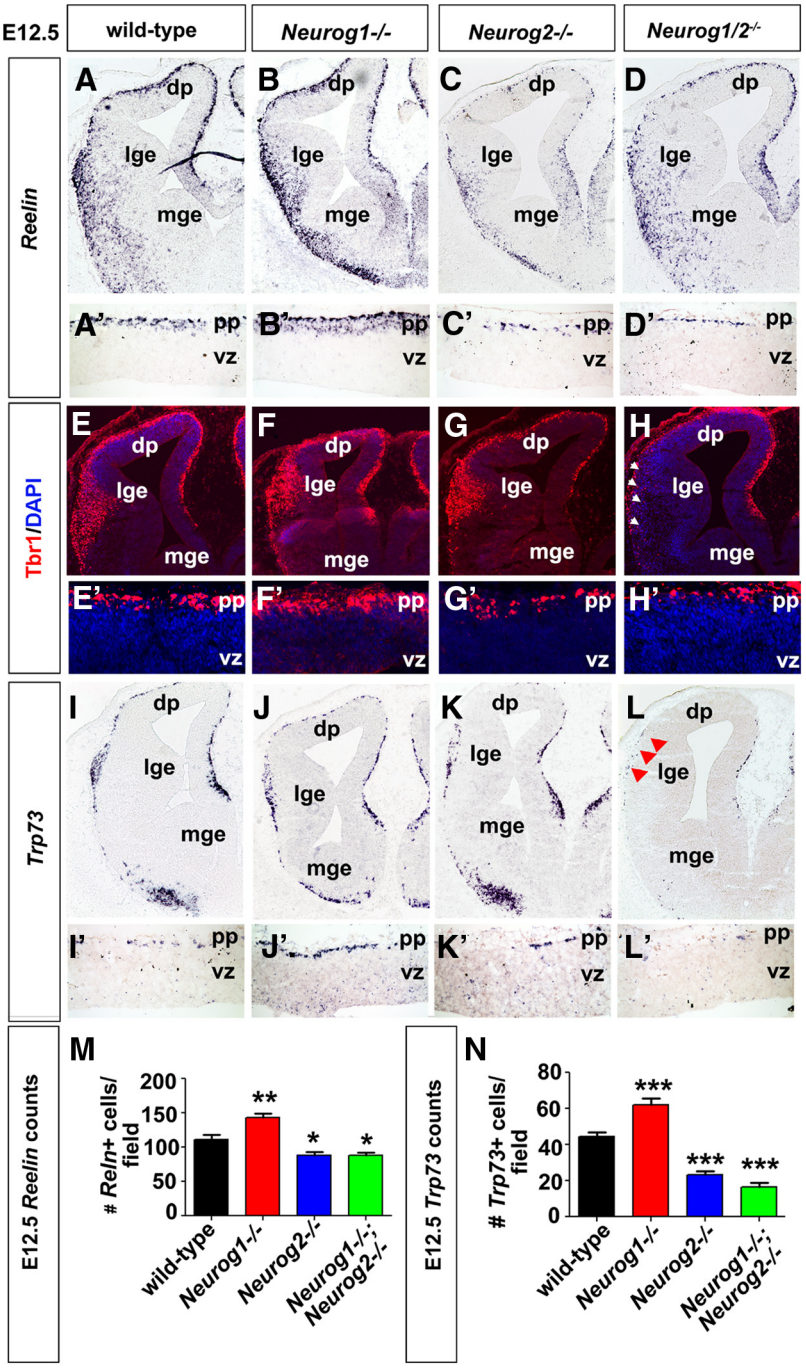

Figure 2. Reduced CR cell differentiation in E12.5 *Neurog2*$^{-/-}$ and *Neurog1/2*$^{-/-}$ neocortices and *Neurog1/2*$^{-/-}$ piriform cortex. ***A–D'***, Expression of *Reelin* in E12.5 wild-type (***A***, ***A'***), *Neurog1*$^{-/-}$ (***B***, ***B'***), *Neurog2*$^{-/-}$ (***C***, ***C'***), and *Neurog1/2*$^{-/-}$ (***D***, ***D'***) cortices. ***A'–D'*** are high-magnification images of ***A–D*** in the neocortical preplate. ***E–H'***, Expression of Tbr1 in E12.5 wild-type (***E***, ***E'***), *Neurog1*$^{-/-}$ (***F***, ***F'***), *Neurog2*$^{-/-}$ (***G***, ***G'***), and *Neurog1/2*$^{-/-}$ (***H***, ***H'***) cortices. ***E'–H'*** are high-magnification images of neocortical preplate in ***E–H***. Arrowheads in ***H*** mark the loss of Tbr1^{+} CR cells in the presumptive piriform cortex. ***I–L'***, Expression of *Trp73* in E12.5 wild-type (***I***, ***I'***), *Neurog1*$^{-/-}$ (***J***, ***J'***), *Neurog2*$^{-/-}$ (***K***, ***K'***), and *Neurog1/2*$^{-/-}$ (***L***, ***L'***) cortices. ***I'–L'*** are high-magnification images of neocortical preplate in ***I–L***. Arrowheads in ***L*** mark the loss of *Trp73*$^{+}$ CR cells in the presumptive piriform cortex. ***M***, ***N***, Quantitation of the number of *Reelin*$^{+}$ (***M***) and *Trp73*$^{+}$ (***N***) cells in the neocortex of embryos for each genotype. Error bars in ***M*** and ***N*** represent SEM. Student's *t* tests were performed comparing all genotypes individually to wild type with *p* values denoted as follows: *$p < 0.05$, **$p < 0.01$, ***$p < 0.005$. dp, Dorsal pallium; lge, lateral ganglionic eminence; mge, medial ganglionic eminence; pp, preplate; vz, ventricular zone.

Defects in CR cell differentiation persist in later stage *Neurog2*$^{-/-}$ and *Neurog1/2*$^{-/-}$ neocortices and piriform cortices

The presence of fewer CR cells in E12.5 *Neurog2*$^{-/-}$ and *Neurog1/2*$^{-/-}$ cortices could be due to a delay rather than a reduction in differentiation. To address this possibility, we examined *Neurog1* and *Neurog2* single and *Neurog1/2* double mutants at E15.5, 3 d after CR cell differentiation is normally complete. At E15.5, *Reln* was expressed in a relatively continuous layer in the neocortical marginal zones of wild-type and *Neurog1*$^{-/-}$ neocortices, whereas distinct gaps in *Reln* expression were detected in *Neurog2*$^{-/-}$ and *Neurog1/*

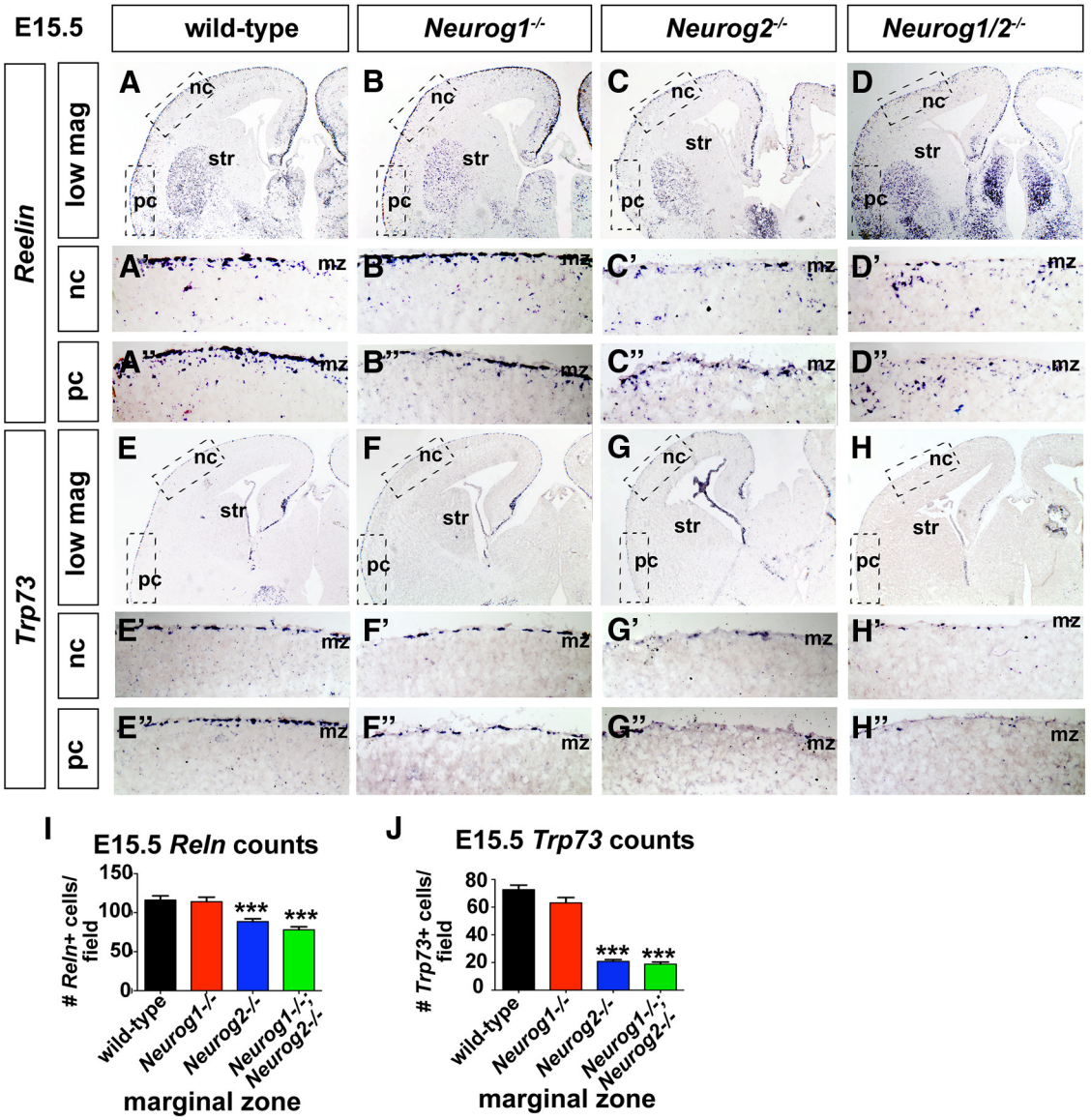

Figure 3. Defects in CR cell differentiation in the E15.5 *Neurog2* $^{-/-}$ neocortex and *Neurog1/2* $^{-/-}$ neocortex and piriform cortex. ***A–D″***, Expression of *Reelin* in E15.5 wild-type (***A–A″***), *Neurog1* $^{-/-}$ (***B–B″***), *Neurog2* $^{-/-}$ (***C–C″***), and *Neurog1/2* $^{-/-}$ (***D–D″***) cortices. ***A′–D′*** are high-magnification images of boxed neocortical regions in ***A–D***. ***A″–D″*** are high-magnification images of boxed piriform cortex regions in ***A–D***. ***E–H″***, Expression of *Trp73* in E15.5 wild-type (***E–E″***), *Neurog1* $^{-/-}$ (***F–F″***), *Neurog2* $^{-/-}$ (***G–G″***), and *Neurog1/2* $^{-/-}$ (***H–H″***) cortices. ***E′–H′*** are high-magnification images of boxed neocortical regions in ***E–H***. ***E″–H″*** are high-magnification images of boxed piriform cortex regions in ***E–H***. ***I***, ***J***, Quantitation of the number of *Reelin* $^{+}$ (***I***) and *Trp73* $^{+}$ (***J***) cells per field in the marginal zone (i.e., CR cells). Error bars represent SEM. Student's *t* tests were performed comparing all genotypes individually to wild type with *p* values denoted as follows: *$p < 0.05$, **$p < 0.01$, ***$p < 0.005$. mz, Marginal zone; nc, neocortex; pc, piriform cortex; str, striatum.

2 $^{-/-}$ mutants (Fig. 3*A–D*'). Accordingly, quantitation of *Reln* $^{+}$ CR cells in the marginal zone revealed 1.3-fold and 1.5-fold reductions, respectively, in *Neurog2* $^{-/-}$ (88.6 ± 3.6 *Reln* $^{+}$ cells/field; $n = 3$; $p = 0.0002$) and *Neurog1/2* $^{-/-}$ (78.1 ± 3.8 *Reln* $^{+}$ cells/field; $n = 2$; $p < 0.0001$) neocortical marginal zones compared with wild-type (116.2 ± 5.4 *Reln* $^{+}$ cells/field; $n = 3$; Fig. 3*I*). *Neurog1* $^{-/-}$ CR numbers had normalized by E15.5 and were not significantly different than in wild-type neocortices (114.1 ± 5.8 *Reln* $^{+}$ cells/field; $n = 3$; $p = 0.79$; Fig. 3*I*). A similar result was observed when analyzing *Trp73* $^{+}$ CR cell numbers, which were reduced 3.4-fold and 3.8-fold, respectively, in *Neurog2* $^{-/-}$ (20.8 ± 1.3 *Trp73* $^{+}$ cells/field; $n = 3$; $p < 0.0001$; Fig. 3*G*,*G*',*J*) and *Neurog1/2* $^{-/-}$ (18.8 ± 1.5 *Trp73* $^{+}$ cells/field; $n = 2$; $p < 0.0001$; Fig. 3*H*,*H*',*J*) neocortical marginal zones compared with wild-type embryos (72.6 ± 3.3 *Trp73* $^{+}$ cells/field; $n = 3$; Fig. 3*E*,*E*',*J*), while *Neurog1* $^{-/-}$ embryos had normal numbers of *Trp73* $^{+}$ cells (63.1 ± 3.9 *Trp73* $^{+}$ cells/field; $n = 3$; $p = 0.07$; Fig. 3*F*,*F*',*J*). Moreover, similar to observations made at E12.5, almost no CR cells were detected in the presumptive piriform cortex of *Neurog1/2* $^{-/-}$ embryos (Fig. 3*D*″,*H*″), whereas CR cells lined the marginal zone of the piriform cortex in all other genotypes (Fig. 3*A*″–*C*″,*E*″–*G*″).

The reduction in CR cell number in *Neurog2* $^{-/-}$ and *Neurog1/2* $^{-/-}$ cortices thus persists at E15.5, and hence is unlikely to be due to a delay in CR cell genesis. Moreover, the original increase in CR cell number observed in E12.5 *Neurog1* $^{-/-}$ cortices is rectified by E15.5, indicating that *Neurog1* is only required to delay cortical neurogenesis at early developmental stages.

Neurog2 is sufficient to induce CR cell differentiation while *Neurog1* limits the formation of neocortical CR cells

The loss of CR cells in *Neurog2* $^{-/-}$ and *Neurog1/2* $^{-/-}$ cortices could arise if the medial signaling domains from which some CR

cells arise are defective (Hanashima et al., 2007; Griveau et al., 2010; Zimmer et al., 2010), or if *Neurog1* and *Neurog2* function as instructive determinants of a CR cell fate. To distinguish between these possibilities, we first examined marker expression in the Fgf-rich pallial septum (Bielle et al., 2005; Zimmer et al., 2010), Wnt/Bmp-rich cortical hem (Takiguchi-Hayashi et al., 2004; Yoshida et al., 2006; García-Moreno et al., 2007; Imayoshi et al., 2008), and Egf-rich ventral pallium (Assimacopoulos et al., 2003). In E12.5 *Neurog1* and *Neurog2* single and *Neurog1/2* double mutant cortices, we observed normal patterns of expression of *Fgf8/17* in the pallial septum (data not shown), *Wnt3a* in the cortical hem (Fig. 4*A–D*; Imayoshi et al., 2008), and *Dbx1* in the ventral pallium (Fig. 4*E–H*). CR cell progenitor domains are thus properly established in *Neurog2*$^{-/-}$ and *Neurog1/2*$^{-/-}$ cortices.

We next asked whether *Neurog1* and *Neurog2* could function as instructive determinants of a CR cell fate. Consistent with this idea, *Neurog2* was previously shown to promote ectopic Reelin expression when misexpressed in the E9.5 choroid plexus (Imayoshi et al., 2008). Here we asked whether *Neurog1* and *Neurog2* were sufficient to promote some or all aspects of a CR cell identity when misexpressed in E10.5 pallial progenitors. Expression vectors for *Neurog1* or *Neurog2* and a pCIG2 vector control, all expressing GFP, were introduced into the E10.5 pallium via *in utero* electroporation (Dixit et al., 2011a). After 2 d of *in vitro* explant culture, cortices were harvested and assessed for the induction of CR marker expression (Fig. 4*I–M*). Consistent with the Imayoshi et al. (2008) study, *Neurog2* was sufficient to induce ectopic Reelin expression in the E10.5 pallium (3.0-fold increase; control: 13.4 ± 2.9% Reelin$^+$GFP$^+$/GFP$^+$ cells; $n = 4$; 567 cells; *Neurog2*: 40.5 ± 4.8% Reelin$^+$GFP$^+$/GFP$^+$; $n = 3$; 1469 cells; $p < 0.005$; Fig. 4*I–M*,*N*). In contrast, *Neurog1* did not induce ectopic Reelin expression and, moreover, *Neurog1* inhibited the ability of *Neurog2* to induce a CR fate when the two genes were coelectroporated (2.3-fold decrease; *Neurog1*: 8.1 ± 3.7% Reelin$^+$GFP$^+$/GFP$^+$ cells; $n = 3$; 79 cells; *Neurog1* plus *Neurog2*: 18.0 ± 4.6% Reelin$^+$GFP$^+$/GFP$^+$; $n = 3$; 757 cells; Fig. 4*N*). In contrast, neither *Neurog1* nor *Neurog2* were sufficient to induce the expression of Trp73 (Fig. 4*P*), even though loss-of-function studies indicate that these proneural genes are required for the generation of *Trp73*$^+$ CR neurons (Figs. 2, 3).

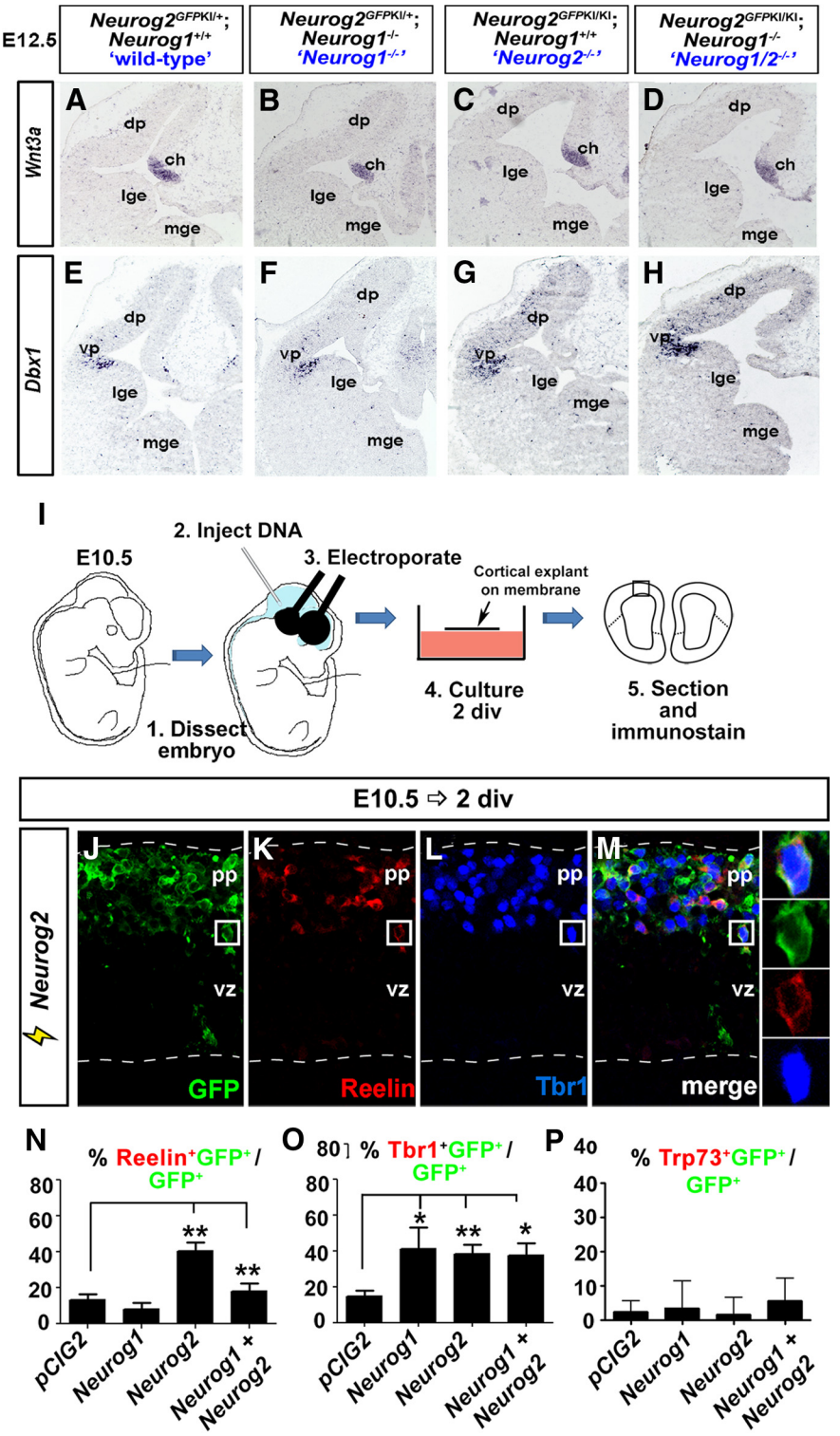

Figure 4. *Neurog1* and *Neurog2* are sufficient to induce the expression of a subset of CR markers. ***A–H***, Expression of *Wnt3a* (***A–D***) and *Dbx1* (***E–H***) in wild-type (***A***, ***E***), *Neurog1*$^{-/-}$ (***B***, ***F***), *Neurog2*$^{-/-}$ (***C***, ***G***), and *Neurog1/2*$^{-/-}$ (***D***, ***H***) E12.5 cortices. ***I***, Schematic representation of *in vitro* electroporation protocol: expression constructs were injected into the E10.5 mouse telencephalon, followed by dissection of the dorsal telencephalon, embryo culture for 2 DIV, and analysis. ***J–M***, Misexpression of *Neurog2-IRES-GFP* in E10.5 cortices, followed after 2 DIV by immunolabeling to visualize expression of GFP (***J***, ***M***, green), Reelin (***K***, ***M***, red), and Tbr1 (***L***, ***M***, blue). Boxes to the right of ***M*** are high-magnification images of the boxed areas in ***J–M***. ***N–P***, Quantitation of the percentage of GFP$^+$ electroporated cells expressing Reelin (***N***), Tbr1 (***O***), or Trp73 (***P***). Error bars represent SEM. Student's *t* tests were performed comparing all genotypes individually to wild type with *p* values denoted as follows: $*p < 0.05$, $**p < 0.01$, $***p < 0.005$. ch, Cortical hem; div, days *in vitro*; dp, dorsal pallium; lge, lateral ganglionic eminence; mge, medial ganglionic eminence; pp, preplate; vz, ventricular zone; vp, ventral pallium.

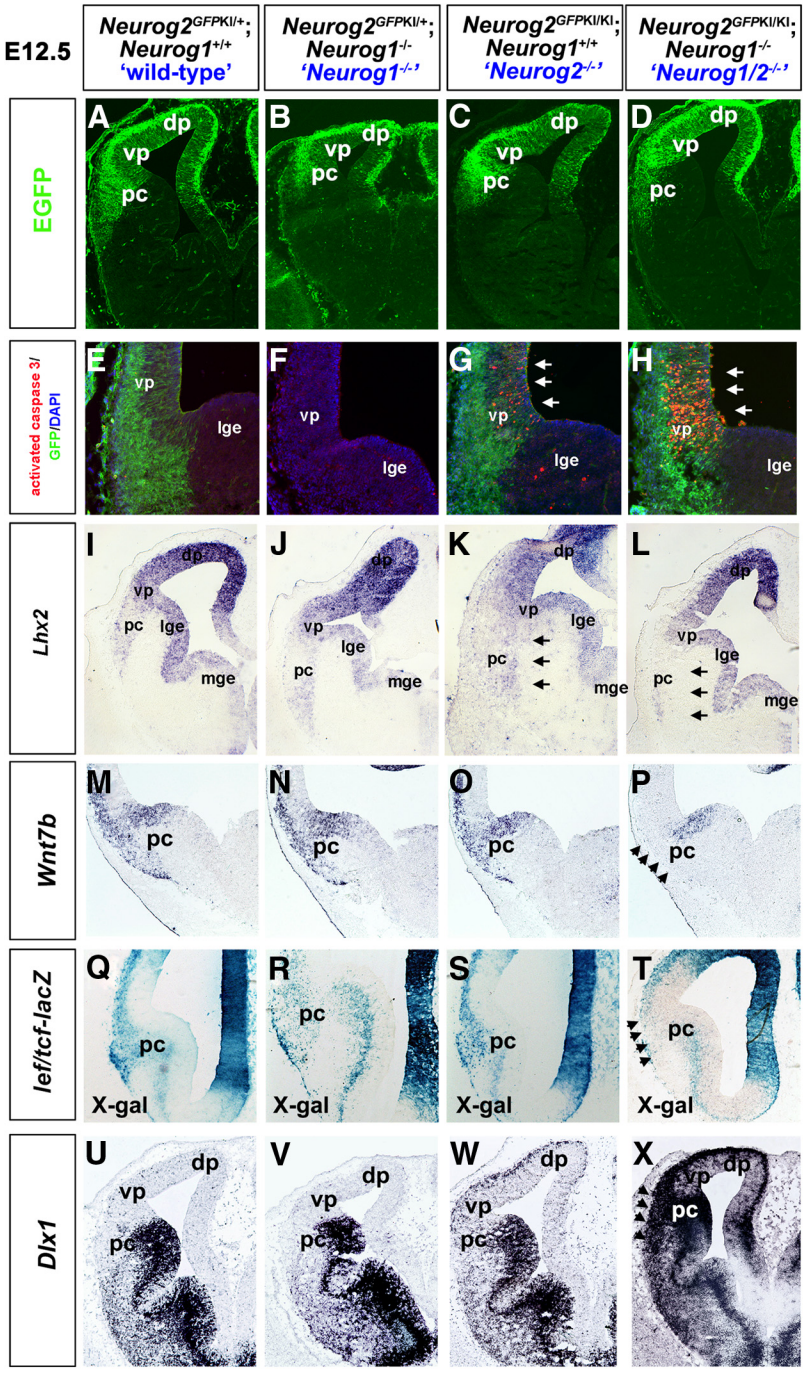

Figure 5. Early defects in cell fate specification in the ventral pallium and presumptive piriform cortex in *Neurog1/2* $^{-/-}$ embryos. ***A–H***, Expression of GFP (***A–D***) and activated caspase 3 (***E–H***, red) in E12.5 *Neurog2*$^{GFP\ KI\ +/-}$ heterozygotes ("wild-type"; ***A***, ***E***), *Neurog1* $^{-/-}$ mutants carrying one copy of the *Neurog2*$^{GFP\ KI}$ allele (***B***, ***F***), *Neurog2*$^{GFP\ KI/KI}$ mutants (***C***, ***G***), and *Neurog1* $^{-/-}$;*Neurog2*$^{GFP\ KI/KI}$ double mutants (*Neurog1/2* $^{-/-}$; ***D***, ***H***). Arrowheads in ***G*** and ***H*** mark elevated levels of apoptosis in the *Neurog2* $^{-/-}$ and *Neurog1/2* $^{-/-}$ ventral pallium. ***I–P***, Expression of Lhx2 (***I–L***) and *Wnt7b* (***M–P***) in E12.5 wild-type (***I***, ***M***), *Neurog1* $^{-/-}$ (***J***, ***N***), *Neurog2* $^{-/-}$ (***K***, ***O***), and *Neurog1/2* $^{-/-}$ (***L***, ***P***) cortices. Arrowheads in ***L*** and ***P*** mark reduced expression of *Lhx2* and *Wnt7b* in the double-mutant ventral pallium. ***Q–T***, X-gal staining (blue) of E12.5 wild-type (***Q***), *Neurog1* $^{-/-}$ (***R***), *Neurog2* $^{-/-}$ (***S***), and *Neurog1/2* $^{-/-}$ (***T***) cortices, all from embryos carrying a *lef/tcf-lacZ* transgene. Arrowhead in ***T*** marks reduced X-gal staining. ***U–X***, Expression of *Dlx1* in E12.5 wild-type (***U***), *Neurog1* $^{-/-}$ (***V***), *Neurog2* $^{-/-}$ (***W***), and *Neurog1/2* $^{-/-}$ (***X***) cortices. Arrowhead in ***X*** marks ectopic *Dlx1* expression in double mutants. dp, Dorsal pallium; lge, lateral ganglionic eminence; pc, piriform cortex; vp, ventral pallium.

The inability of *Neurog1* to promote a CR cell fate is not at first glance consistent with our loss-of-function studies, which suggest that *Neurog1* can promote a CR cell fate in the absence of *Neurog2*. One possibility is that *Neurog1* can induce some aspects of a CR cell fate, such as a cortical-specific neuronal identity, and not subtype-specific CR pathways, a mode of action that would be consistent with *Neurog1*'s partial fate specification properties in the OE (Cau et al., 2002). To test this model, we asked whether *Neurog1* and *Neurog2* could induce the expression of Tbr1, a cortical identity marker. In striking contrast to Reelin, both *Neurog1* and *Neurog2* induced ectopic Tbr1 expression whether expressed together or apart (2.8-fold, 2.6-fold, and 2.5-fold increases respectively; control vector: 14.8 ± 3.0% Tbr1$^+$GFP$^+$/GFP$^+$; $n = 4$; 251 cells; *Neurog1*: 41.3 ± 12.0% Tbr1$^+$GFP$^+$/GFP$^+$; $n = 3$; 140 cells; $p < 0.05$ vs pCIG2; *Neurog2*: 38.6 ± 4.9% Tbr1$^+$GFP$^+$/GFP$^+$; $n = 3$; 923 cells; $p < 0.005$ vs pCIG2; *Neurog1* plus *Neurog2*: 37.7 ± 6.6% Tbr1$^+$GFP$^+$/GFP$^+$; $n = 3$; 806 cells; $p < 0.05$ vs pCIG2; Fig. 4*O*).

Thus, while *Neurog2* is sufficient to promote the expression of cortical and some CR cell identity markers in early pallial progenitors, as previously shown in the choroid plexus (Imayoshi et al., 2008), *Neurog1* is only sufficient to induce a cortical identity, at least in the cellular context and time frame tested. Moreover, *Neurog1* impedes *Neurog2*'s ability to induce CR marker expression, consistent with a role for this factor in controlling the rate of early CR cell production.

Early defects in cell fate specification and not migration in the *Neurog1/2* $^{-/-}$ piriform cortex

Neurog2 has sequential functions in the neocortex: first promoting a CR identity and later specifying deep-layer neocortical cell fates. We thus asked whether *Neurog1* and *Neurog2* have similar sequential functions in the ventral pallium/piriform cortex. After forming CR cells, ventral pallial progenitors give rise to neurons in the piriform cortex, with layer I lot cells differentiating between E10 and E11, followed by deep-layer III neurons at E12, and layer II neurons arising between E13 and E14 (de Carlos et al., 1996; Tomioka et al., 2000; Hirata et al., 2002; Vyas et al., 2003). To first determine whether *Neurog2*-expressing progenitors in the ventral pallium populate the piriform cortex, we examined GFP expression in E12.5 "wild-type" (i.e., *Neurog2*$^{GFP\ KI/+}$ heterozygous) and *Neurog1* and *Neurog2* single and double mutant embryos carrying a *Neurog2*$^{GFP\ KI}$ allele (Fig. 5*A–D*). In E12.5 *Neurog2*$^{GFP\ KI\ +/-}$ heterozygotes, GFP$^+$ cells emanated from the ventral pallium, accumulating in a ventrolateral wedge adjacent to the LGE in the nascent piriform cortex (Fig. 5*A*). The accumulation of GFP$^+$

cells in a wedge shape in the piriform cortex closely mimicked the spatial pattern of Tbr1$^+$ and Trp73$^+$ cells observed above (Fig. 2*E*,*I*). A similar ventrolateral stream of GFP$^+$ cells was also observed in *Neurog1*$^{-/-}$ mutants carrying one copy of the *Neurog2*$^{GFP\,KI}$ allele, in *Neurog2*$^{GFP\,KI/KI}$ single mutants, and in *Neurog1*$^{-/-}$;*Neurog2*$^{GFP\,KI/KI}$ double mutants (Fig. 5*B–D*). Thus, the tangential migration of neurons derived from the ventral pallium into the piriform cortex is not grossly perturbed by the loss of *Neurog1* and *Neurog2.* However, immunostaining with anti-activated caspase 3 revealed that there is elevated levels of apoptosis in the *Neurog2*$^{-/-}$ and *Neurog1/2*$^{-/-}$ ventral pallium at E12.5, after CR cell production has ended and the genesis of piriform cortical neurons has begun (Fig. 5*E–H*). To test whether cells with a piriform cortex identity were selectively lost in *Neurog2*$^{-/-}$ and *Neurog1/2*$^{-/-}$ cortices, we examined the expression of *Lhx2,* a cortical selector gene that regulates a key decision between making neocortical versus piriform cortical structures (Chou et al., 2009). In E12.5 wild-type and *Neurog1*$^{-/-}$ cortices (Fig. 5*I*,*J*), a stream of *Lhx2*$^+$ cells emanated ventrally from the ventral pallium, marking the presumptive piriform cortex. In contrast, the *Lhx2*$^+$ presumptive piriform cortical neurons were disorganized in *Neurog2*$^{-/-}$ embryos and, strikingly, were lost in *Neurog1/2*$^{-/-}$ cortices (Fig. 5*K*,*L*).

To further assess piriform cortex development in E12.5 *Neurog1* and *Neurog2* single and double mutants, we monitored canonical Wnt signaling, which specifies a dorsal telencephalic cell fate (Gunhaga et al., 2003; Hirabayashi et al., 2004; Israsena et al., 2004; Backman et al., 2005; Machon et al., 2005; Watanabe et al., 2005). *Wnt7b,* which can initiate canonical signaling (Wang et al., 2005), was expressed in neurons migrating into the outer layers of the developing piriform cortex in E12.5 wild-type, *Neurog1*$^{-/-}$, and *Neurog2*$^{-/-}$ embryos (Fig. 5*M–P*). In contrast, *Wnt7b* expression was strikingly absent in the presumptive *Neurog1/2*$^{-/-}$ piriform cortex, although transcripts were still detected in the dorsal LGE (Fig. 5*P*). To further test whether canonical Wnt signaling was indeed disrupted, we monitored β-galactosidase activity in a transgenic line carrying a *lef/tcf-lacZ* reporter (Mohamed et al., 2004). In E12.5 wild-type, *Neurog1*$^{-/-}$, and *Neurog2*$^{-/-}$ embryos, *lef/tcf-lacZ* reporter activity was detected throughout the wedge of cells corresponding to the presumptive piriform cortex (Fig. 5*Q–T*). In contrast, the presumptive piriform cortex in E12.5 *Neurog1/2*$^{-/-}$ embryos was devoid of *lef/tcf-lacZ* reporter activity, indicating that canonical Wnt signaling was strongly reduced in the *Neurog1/2*$^{-/-}$ piriform cortex (Fig. 5*T*). Finally, to test whether loss of a dorsal telencephalic identity was due to a transition to a ventral fate, we examined the expression of *Dlx1*. *Dlx1* was ectopically expressed throughout the *Neurog1/2*$^{-/-}$ piriform cortex (Fig. 5*U–X*), as previously shown in adjacent neocortical territories (Fode et al., 2000; Schuurmans et al., 2004).

Thus, the loss of both *Neurog1* and *Neurog2* does not prevent the migration of neurons derived from the ventral pallium into the presumptive piriform cortex, but rather results in a ventralization of these cells, which may contribute to their subsequent death.

Lamination and cell fate specification defects in *Neurog1/2*$^{-/-}$ piriform cortex

To further characterize defects in piriform cortex development in *Neurog1/2*$^{-/-}$ embryos, we first examined histological sections at E18.5, when neurogenesis and lamination are essentially complete. In E18.5 wild-type, *Neurog1*$^{-/-}$, and *Neurog2*$^{-/-}$ brains, the transition from a six-layered neocortex to three-layered piriform cortex was evident as a medial inflection and narrowing of the densely stained neuronal layers (Fig. 6*A–C*). In contrast, in E18.5 *Neurog1/2*$^{-/-}$ brains, the presumptive piriform cortex was thinner, hypocellular, and lacked densely stained neuronal layers (Fig. 6*D*).

To examine the basis of these histological defects, we used markers to label the different layers of the piriform cortex. In E15.5 wild-type, *Neurog1*$^{-/-}$, and *Neurog2*$^{-/-}$ embryos, Tbr1, which marks neocortical and piriform cortical neurons (Hevner et al., 2001), was expressed in all three layers of the piriform cortex (Fig. 6*E–G*). In contrast, many fewer neurons expressed Tbr1 in the E15.5 *Neurog1/2*$^{-/-}$ piriform cortex (Fig. 6*H*), which is consistent with a similar reduction observed at E12.5 (Fig. 2*H*). Similarly, the expression of *Ctip2*, which was expressed in layer II of the E15.5 wild-type, *Neurog1*$^{-/-}$, and *Neurog2*$^{-/-}$ piriform cortex, as well as *Id2,* which was expressed in layers II and III, were both strongly reduced in the *Neurog1/2*$^{-/-}$ piriform cortex (Fig. 6*I–P*). The loss of piriform cortex marker expression in *Neurog1/2*$^{-/-}$ embryos was not due to a transformation from a piriform to neocortical identity, as *Fezf1* and *Tle4*, which mark upper and deep layer neocortical neurons, respectively, and which are not expressed in the piriform cortex, were not ectopically expressed in the presumptive piriform cortex of *Neurog1/2*$^{-/-}$ embryos (data not shown).

While the piriform cortex has a ventral location, it has a dorsal origin, arising from lateral and ventral pallial progenitors. We thus reasoned that the loss of "dorsal" (cortical)-specific marker expression in the *Neurog1/2*$^{-/-}$ piriform cortex could be due to a dorsal-to-ventral fate transition, resulting in the generation of ectopic interneurons, as previously shown in *Neurog2*$^{-/-}$ and *Neurog1/2*$^{-/-}$ neocortices (Fode et al., 2000; Schuurmans et al., 2004) and OBs (Shaker et al., 2012). We thus examined the expression of *Etv1* and Pax6, which label dopaminergic periglomerular interneurons in the OB (Stenman et al., 2003; Kohwi et al., 2005; Saino-Saito et al., 2007), and *Dlx1,* which labels GABAergic interneurons in both the cortex and OB (Anderson et al., 1997; Long et al., 2007). All three interneuron markers were ectopically expressed in E15.5 *Neurog2*$^{-/-}$ and *Neurog1/2*$^{-/-}$ piriform cortices, whereas only scattered piriform cortex interneurons expressed these markers in E15.5 wild-type and *Neurog1*$^{-/-}$ embryos (Fig. 6*Q–Z*,*A*',*B*'). However, neuronal misspecification was much more severe in the double-mutant piriform cortex, with ectopic *Etv1* and Pax6 expression detected in all three layers (Fig. 6*T*,*B*'), while ectopic *Dlx1* expression was restricted to deep layer III (Fig. 6*X*).

Together, these results suggest that the *Neurog1/2*$^{-/-}$ piriform cortex is comprised of neurons with aberrant molecular identities. Strikingly, the "ventralized" neurons have a similar molecular signature as OB interneurons, which are derived from the dorsal LGE, a subpallial progenitor domain that lies immediately adjacent to the ventral pallium (Vergaño-Vera et al., 2006; Flames and Hobert, 2009).

LOT formation is perturbed in the *Neurog1/2*$^{-/-}$ double-mutant piriform cortex

The piriform cortex is part of a three-part neural network that also includes the OE and OB, which together mediate the primary sense of olfaction. We previously showed that *Neurog1/2*$^{-/-}$ double mutants only form a remnant of an OB-like structure (OBLS) in an aberrant ventral position (Shaker et al., 2012). Nevertheless, despite this abnormal architecture, some glutamatergic mitral cells, which are the output neurons of the OB that target the piriform cortex, differentiate in the *Neurog1/2*$^{-/-}$ OBLS (Shaker et al., 2012). We therefore questioned whether *Neurog1/2*$^{-/-}$ mitral cell axons are capable of forming a LOT that innervates the piriform cortex.

To trace LOT axons, a DiI crystal was inserted into the OB of E18.5 wild-type and *Neurog1* and *Neurog2* single-mutant and

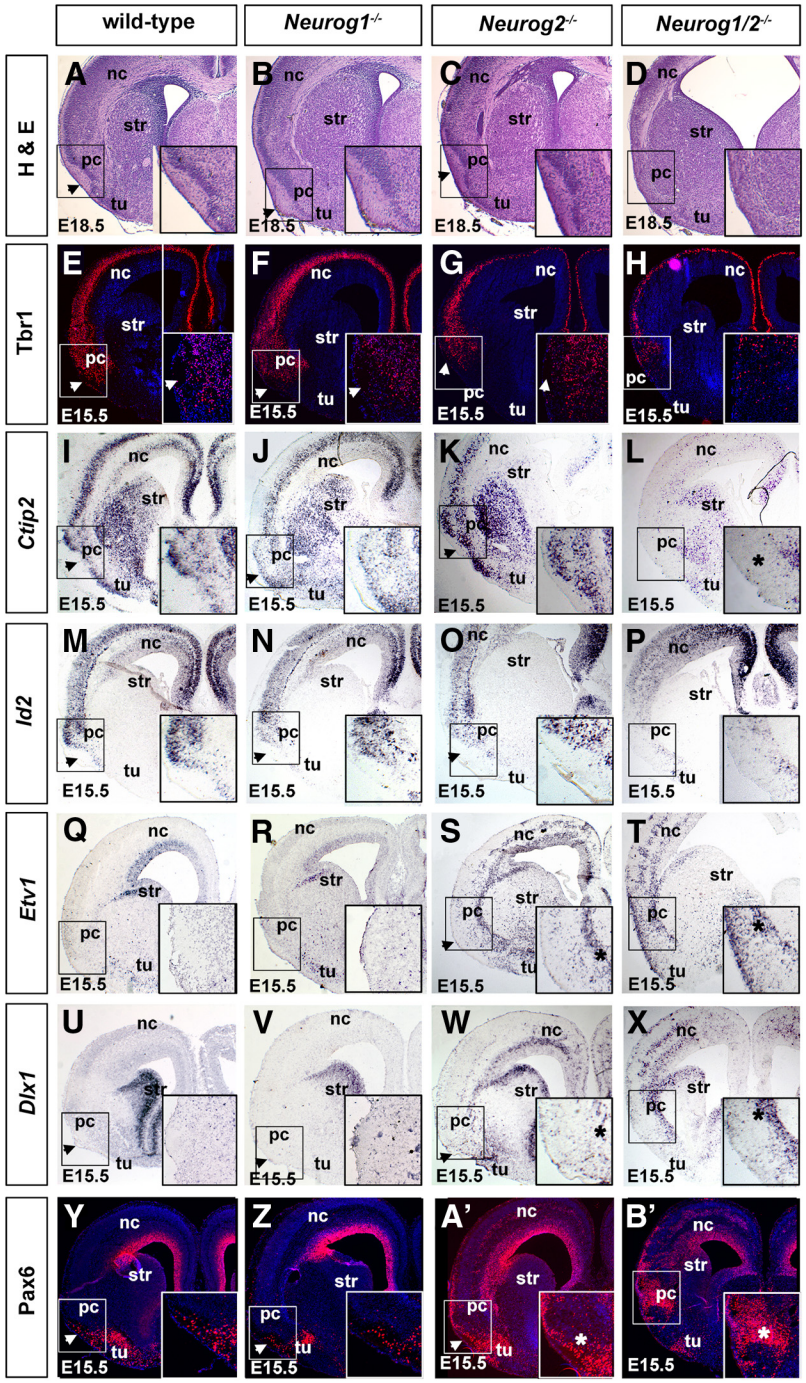

Figure 6. Defects in lamination and cell fate specification in the *Neurog1/2* $^{-/-}$ piriform cortex. ***A–D***, Hematoxylin and eosin staining of E18.5 wild-type (***A***), *Neurog1* $^{-/-}$ (***B***), *Neurog2* $^{-/-}$ (***C***), and *Neurog1/2* $^{-/-}$ (***D***) cortices. Arrowheads in ***A–C*** mark site of LOT formation. ***E–Z, A′, B′***, Expression of Tbr1 (***E–H***), *Ctip2* (***I–L***), *Id2* (***M–P***), *Etv1* (***Q–T***), *Dlx1* (***U–X***), and Pax6 (***Y, Z, A′, B′***) in E15.5 wild-type (***E, I, M, Q, U, Y***), *Neurog1* $^{-/-}$ (***F, J, N, R, V, Z***), *Neurog2* $^{-/-}$ (***G, K, O, S, W, A′***), and *Neurog1/2* $^{-/-}$ (***H, L, P, T, X, B′***) cortices. Insets in ***I–P*** are high-magnification images of the piriform cortex. Asterisks in ***L*** and ***P*** show reduced expression of *Ctip2* and *Id2* in the *Neurog1/2* $^{-/-}$ piriform cortex. Arrowheads in ***S, T, W, X, A′***, and ***B′*** mark the ectopic expression of *Etv1*, *Dlx1*, and Pax6 in *Neurog2* $^{-/-}$ and *Neurog1/2* $^{-/-}$ piriform cortices. nc, Neocortex; pc, piriform cortex; str, striatum; tu, olfactory tubercle.

double-mutant embryos (Fig. 7*A–D*). In E18.5 wild-type embryos, DiI-labeled LOT axons formed a narrow axon bundle that extended along the lateral surface of the telencephalon before turning in a ventral direction to innervate the piriform cortex (Fig. 7*A*). DiI crystals inserted into the *Neurog1* $^{-/-}$ OB also anterogradely labeled the LOT (Fig. 7*B*), even though the *Neurog1* $^{-/-}$ OB is smaller and abnormally laminated (Shaker et al., 2012). Likewise, *Neurog2* $^{-/-}$ mitral cells, which differentiate normally (Shaker et al., 2012), also formed a LOT (Fig. 7*C*). In contrast, in E18.5 *Neurog1/2* $^{-/-}$ brains, DiI crystals placed in the rostroventral telencephalon did not label a distinct LOT, suggesting that the ectopically localized mitral cells in the *Neurog1/2* $^{-/-}$ OBLS failed to extend axons to innervate the piriform cortex (Fig. 7*D*).

To confirm that LOT formation did not occur in *Neurog1/2* $^{-/-}$ embryos, we examined calretinin expression. Calretinin immunolabeling was detected in mitral cell axon bundles innervating the piriform cortex in E15.5 wild-type, *Neurog1* $^{-/-}$, and *Neurog2* $^{-/-}$ brains (Fig. 7*E–H′*). In contrast, a calretinin $^{+}$ axonal bundle was not observed in the presumptive piriform cortex in *Neurog1/2* $^{-/-}$ mutants (Fig. 7*H*,*H′*). To further examine LOT formation, we examined embryos carrying a *Neurog2*$^{GFP\,KI}$ allele, which serves as a short-term lineage trace of glutamatergic projection neurons in both the neocortex and OB (Britz et al., 2006; Shaker et al., 2012). A distinct GFP $^{+}$ LOT was observed in the piriform cortex of *Neurog2*$^{GFP\,KI\,+/-}$ heterozygotes (Fig. 7*I*,*M*, *Q*), as well as in *Neurog1* $^{-/-}$ mutants carrying one copy of the *Neurog2*$^{GFP\,KI}$ allele (Fig. 7*J*,*N*,*R*) and *Neurog2*$^{GFP\,KI/KI}$ single mutants (Fig. 7*K*,*O*,*S*). In contrast, a GFP $^{+}$ LOT was not evident in the *Neurog1* $^{-/-}$; *Neurog2*$^{GFP\,KI/KI}$ piriform cortex (Fig. 7*L*,*P*,*T*). Notably, the LOT, which is comprised of mitral cell axons, was also distinguishable in wild-type, *Neurog1* $^{-/-}$, and *Neurog2* $^{-/-}$ piriform cortex by the absence of MAP2 expression, which is a dendritic marker (Fig. 7*M–O*), whereas a MAP2-free zone was not observed in the presumptive *Neurog1/2* $^{-/-}$ piriform cortex (Fig. 7*P*). Thus, although some mitral cells differentiate in the *Neurog1/2* $^{-/-}$ OBLS, they fail to innervate the piriform cortex.

Defects in the differentiation of lot1 guidepost neurons in the *Neurog1/2* $^{-/-}$ piriform cortex

LOT formation depends on lot guidepost cells, which have a dorsal pallial origin (Sato et al., 1998; Tomioka et al., 2000). We speculated that the failure of LOT formation in the *Neurog1/2* $^{-/-}$ piriform cortex could be due to defects in the differentiation of lot cells, which could be derived from a *Neurog2*-lineage. To monitor lot cell formation, we took advantage of two markers: a lot-cell-specific monoclonal antibody called lot1 (Sato et al., 1998), which recently was shown to recognize metabotropic glutamate receptor subtype-1 (mGluR1), and an *mGluR1* riboprobe (Hirata et al., 2012). To first determine whether lot cells were derived from the *Neurog2* lineage,

we performed lot1 immunolabeling on embryos carrying a *Neurog2*$^{GFP\,KI}$ allele. In E12.5 *Neurog2*$^{GFP\,KI\,+/-}$ heterozygotes (wild type), *Neurog1*$^{-/-}$ mutants carrying one copy of the *Neurog2*$^{GFP\,KI}$ allele, *Neurog2*$^{GFP\,KI/KI}$ single mutants, and *Neurog2*$^{GFP\,KI/KI}$; *Neurog1*$^{-/-}$ double mutants, lot1 and GFP were coexpressed (Fig. 8*A–C*). However, in *Neurog1/2*$^{-/-}$ embryos, many fewer lot1^{+} cells migrated into the presumptive piriform cortex compared with all other genotypes (Fig. 8*D*). Similarly, *mGluR1* was expressed in the presumptive piriform cortex in E12.5 wild-type, *Neurog1*$^{-/-}$, and *Neurog2*$^{-/-}$ piriform cortex, whereas many fewer *mGluR1*$^{+}$ lot cells were detected in *Neurog1/2*$^{-/-}$ embryos (Fig. 8*E–H*). Expression of lot1 persisted in the piriform cortex at E15.5, with notable defects only observed in *Neurog1/2*$^{-/-}$ piriform cortex (Fig. 8*I–L*'). The differentiation of lot cells is thus strikingly reduced in *Neurog1/2*$^{-/-}$ embryos.

We were struck by the similarities in the E12.5 expression profiles of lot1 (Fig. 8*A–D*) and *Trp73* (Fig. 2*I–L*), which labels a subset of CR cells (Meyer et al., 2002, 2004). Given their similarities, we speculated that lot guidepost cells could be a subpopulation of CR neurons. While previous studies have suggested that there is limited overlap in the expression of lot1 and Reelin (Sato et al., 1998), in our studies, which were conducted on sections instead of in whole-mount, we found that a subset of E12.5 lot1^{+} cells indeed coexpressed Reelin (Fig. 8*M*,*N*,*N*′) and Trp73, the full-length Trp73 isoform (Fig. 8*O*,*P*,*P*'). Moreover, quantitation of coexpression rates revealed that the high lot1^{+} cells that surround the LOT frequently coexpressed Reelin (94.5 ± 0.8%, $n = 3$, 697 cells) and Trp73 (96.0 ± 1.2%, $n = 3$, 1068 cells), while the lower-expressing lot1^{+} cells that are farther away from the LOT displayed reduced levels of Reelin (39.6 ± 4.0%, $n = 3$, 2228 cells) and Trp73 (43.5 ± 4.2%, $n = 3$, 2218 cells) coexpression (Fig. 8*Q*).

We thus conclude that lot guidepost cells are a subset of CR neurons, revealing that these cells have a pallial origin, and depend on both *Neurog1* and *Neurog2* for their differentiation (Fig. 8*R*,*S*).

Trp73 is required for LOT formation and lot cell positioning

We reasoned that if lot cells were indeed a subpopulation of Reelin^{+}/Trp73^{+} CR neurons, that the mutation of *Reelin* and/or *Trp73* could in turn influence lot cell formation and/or function. Indeed, *Reelin* is required for cellular orientation of neocortical layer VI neurons (O'Dell et

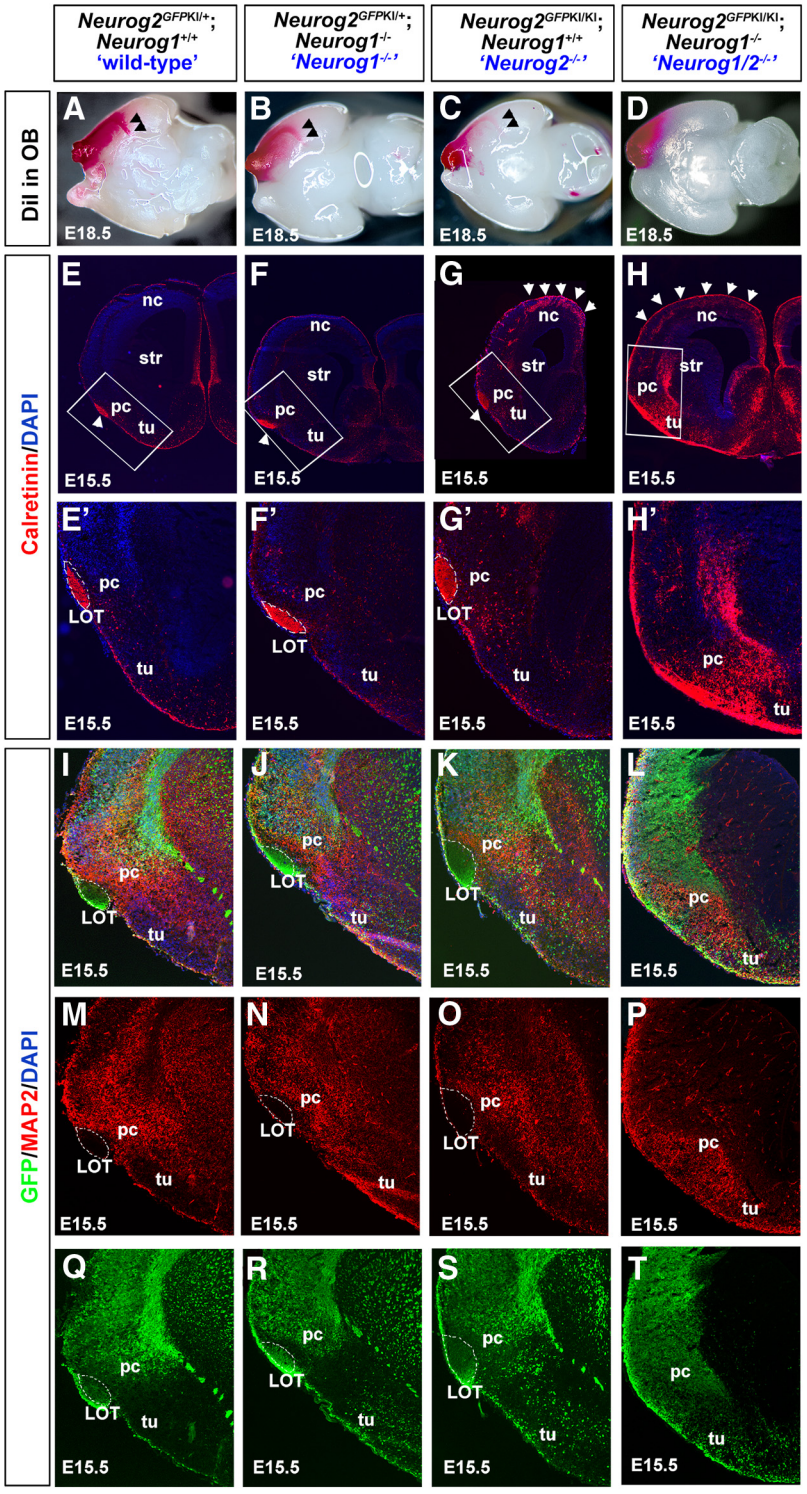

Figure 7. LOT formation is perturbed in the *Neurog1/2*$^{-/-}$ piriform cortex. ***A–D***, LOT axons were traced by inserting a DiI crystal into E18.5 wild-type (***A***), *Neurog1*$^{-/-}$ (***B***), *Neurog2*$^{-/-}$ (***C***), and *Neurog1/2*$^{-/-}$ (***D***) OBs. Arrowheads mark the ventromedial turn of the forming LOT, which fails to form in *Neurog1/2*$^{-/-}$ embryos. ***E–H′***, Labeling of OB mitral cell axons in the LOT with anti-calretinin in E15.5 wild-type (***E***, ***E′***), *Neurog1*$^{-/-}$ (***F***, ***F′***), *Neurog2*$^{-/-}$ (***G***, ***G′***), and *Neurog1/2*$^{-/-}$ (***H***, ***H′***) piriform cortices. Blue is a DAPI counterstain. ***E′–H′*** are higher-magnification images of boxed areas in ***E–H***. Arrowheads in ***G*** and ***H*** mark supernumerary calretinin^{+} interneurons in *Neurog2*$^{-/-}$ and *Neurog1/2*$^{-/-}$ neocortices, respectively. ***I–T***, Expression of GFP (green) and MAP2 (red) in E15.5 *Neurog2*$^{GFP\,KI\,+/-}$ heterozygotes ("wild-type"; ***I***, ***M***, ***Q***), *Neurog1*$^{-/-}$ mutants carrying one copy of the *Neurog2*$^{GFP\,KI}$ allele (***J***, ***N***, ***R***), *Neurog2*$^{GFP\,KI/KI}$ mutants (***K***, ***O***, ***S***), and *Neurog1*$^{-/-}$;*Neurog2*$^{GFP\,KI/KI}$ double mutants (*Neurog1/2*$^{-/-}$; ***L***, ***P***, ***T***). Blue is a DAPI counterstain. The dotted white line outlines the LOT. nc, Neocortex; pc, piriform cortex; str, striatum; tu, olfactory tubercle.

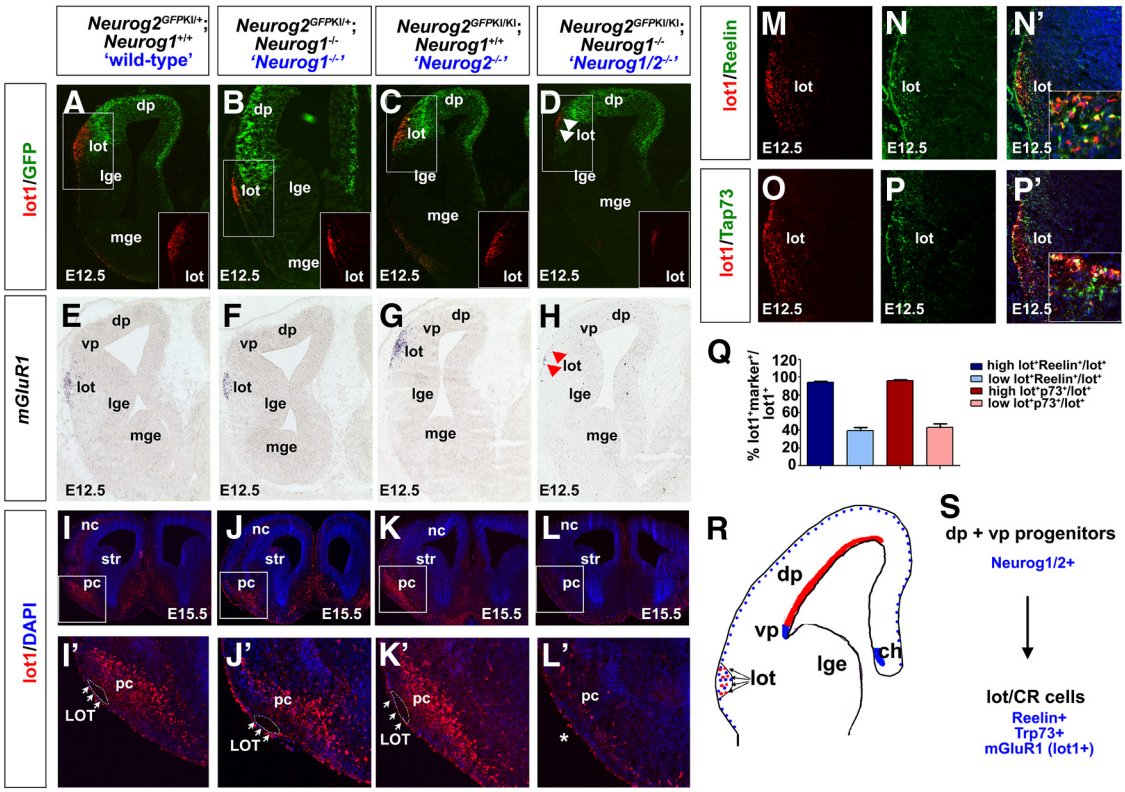

Figure 8. Lot cells, which are reduced in number in the *Neurog1/2* $^{-/-}$ piriform cortex, are a subpopulation of CR cells. ***A–H***, Labeling of E12.5 telencephalons from *Neurog2*$^{GFP\ KI}$ $^{+/-}$ heterozygotes ("wild-type"; ***A***, ***E***), *Neurog1* $^{-/-}$ mutants carrying one copy of the *Neurog2*$^{GFP\ KI}$ allele (***B***, ***F***), *Neurog2*$^{GFP\ KI/KI}$ mutants (***C***, ***G***), and *Neurog1* $^{-/-}$;*Neurog2*$^{GFP\ KI/KI}$ double mutants (*Neurog1/2* $^{-/-}$; ***D***, ***H***) with anti-lot1 (***A–D***, red), anti-GFP (***A–D***, green), and a *mGluR1* riboprobe (***E–H***). Insets in ***A–D*** are lot1 immunostaining of the lot. Arrows in ***D*** and ***H*** mark a loss of lot cells in the *Neurog1/2* $^{-/-}$ piriform cortex. (***I–L′***) Expression of lot1 in E15.5 wild-type (***I***, ***I′***), *Neurog1* $^{-/-}$ (***J***, ***J′***), *Neurog2* $^{-/-}$ (***K***, ***K′***), and *Neurog1/2* $^{-/-}$ (***L***, ***L′***) cortices. The images in ***I′–L′*** are high-magnification images of the boxed areas in ***I–L***. ***M–P***, Coexpression of lot1 (***M***, ***N′***, red) and Reelin (***N***, ***N′***, green), and of lot1 (***O***, ***P′***, red) and Trp73 (***P***, ***P′***) in the lot. Blue is DAPI counterstain in ***N′*** and ***P′***. Insets in ***N′*** and ***P′*** are higher-magnification images of the lot. ***Q***, Quantitation of the coexpression of lot1 with Reelin and Trp73. Cells that expressed high levels of lot1, which surround the LOT, were counted separately from those displaced from the lot (high and low lot $^{+}$ cells, respectively). ***R***, Schematic representation of E12.5 telencephalon, depicting the suggested dorsal pallial source of lot cells (red), and the cortical hem and ventral pallium as the sites of CR cell genesis (blue). ***S***, Summary of our findings, demonstrating that *Neurog1* and *Neurog2* are coexpressed in dorsal and ventral pallial progenitors, which give rise to lot cells, a subset of Reelin $^{+}$/Trp73 $^{+}$ CR cells. ch, Cortical hem; dp, dorsal pallium; lge, lateral ganglionic eminence; lot, lot guidepost cells; vp, ventral pallium.

al., 2012), while *Trp73* is required for CR cell genesis (Meyer et al., 2004). Notably, *Trp73* has two transcriptional start sites, and it is only the larger TAp73 protein, which is generated via transcription from an upstream P1 promoter, that is a functional transcription factor (Conforti et al., 2012). Moreover, the TAp73 isoform regulates the expression of Hey2, a repressor of bHLH proteins, such as *Neurog1* and *Neurog2* (Sakamoto et al., 2003; Fujitani et al., 2010). Thus, to test whether genes involved in CR genesis and/or function also influenced lot formation, we analyzed E15.5 *Reeler*, *Trp73* $^{-/-}$ (*p73* $^{-/-}$), and *TAp73* $^{-/-}$ cortices.

We first examined whether CR cell production was affected in these mutants. Interestingly, while the expression of Trp73 in neocortical and cortical CR cells appeared normal in E15.5 *Reeler* mutants (Fig. 9*A*,*B*), the expression of *Reelin* was strikingly reduced in the *p73* $^{-/-}$ and *TAp73* $^{-/-}$ piriform cortical and neocortical marginal zones (Fig. 9*C–E*), which is consistent with previous studies (Meyer et al., 2002, 2004). Thus, if CR cells remain in *p73* $^{-/-}$ and *TAp73* $^{-/-}$ cortices, they have an abnormal molecular identity.

Next we examined whether LOT formation, which depends on lot cells (Sato et al., 1998), was disrupted in the absence of *Reelin* and *p73*. Strikingly, calretinin immunolabeling marked a larger and less clearly defined LOT in both *p73* $^{-/-}$ and *TAp73* $^{-/-}$ piriform cortices (Fig. 9*H–J*,*M–O*), whereas LOT formation was normal in *Reeler* mutants (Fig. 9*F*,*G*,*K*,*L*,*O*). In addition, the borders of the LOT were not well circumscribed in *p73* $^{-/-}$ and *TAp73* $^{-/-}$ piriform cortices. Instead, DAPI $^{+}$ cells were found within the interior of the LOT (Fig. 9*K–N*,*T*). Furthermore, immunostaining with lot1 revealed that lot guidepost cells were in some instances aberrantly localized within the LOT in *p73* $^{-/-}$ and *TAp73* $^{-/-}$ mutants (Fig. 9*M*,*N*,*R–T*), whereas lot1 $^{+}$ cells were rarely observed in the LOT in wild-type or *Reeler* mutant cortices (Fig. 9*K*,*L*,*P*,*Q*,*T*).

Thus, not only is Trp73 expressed in lot cells, which are a subpopulation of CR neurons, but *p73* is also required for the proper organization of lot cells, and for the subsequent innervation of the piriform cortex by LOT axons.

Discussion

The cerebral cortex is comprised of the archicortex, neocortex, and piriform cortex, each derived from distinct pallial progenitor domains during development. Within each pallial territory, progenitor cells undergo temporal identity transitions, so that the diverse neuronal populations that make up each cortical structure are generated at their correct times and in proper numbers. Here we demonstrate that the proneural genes *Neurog1* and *Neurog2* form a regulatory loop to temporally control successive cell fate decisions in the ventral pallium. At early stages, either *Neurog1* or *Neurog2* are required to specify a CR cell identity. In addition, *Neurog1* has an added early role—preventing preco-

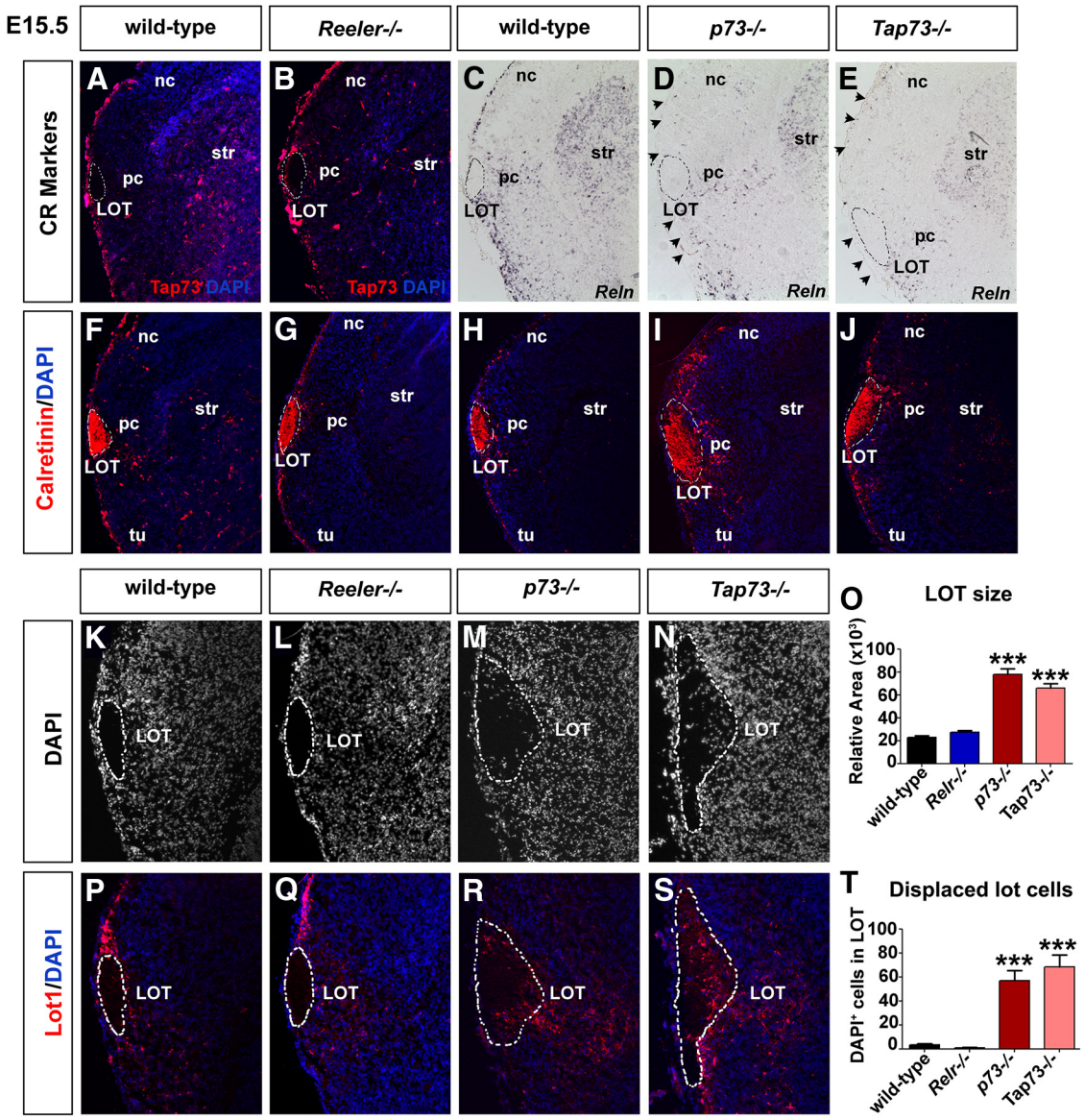

Figure 9. Defects in LOT formation and lot cell positioning in *p73* and *TAp73* mutants. ***A–J***, Expression of Trp73 (***A***, ***B***), *Reelin* (***C***, ***D***), and calretinin (***F–J***) in E15.5 wild-type (***A***, ***C***, ***F***, ***H***), *Reeler* $^{-/-}$ (***B***, ***G***), *p73* $^{-/-}$ (***D***, ***I***), and *TAp73* $^{-/-}$ (***E***, ***J***) cortices. ***K–T***, DAPI staining (***K–N***; ***P–S***, blue counterstain) and lot1 immunolabeling (***P–S***, red label) of E15.5 wild-type (***K***, ***P***), *Reeler* $^{-/-}$ (***L***, ***Q***), *p73* $^{-/-}$ (***M***, ***R***), and *TAp73* $^{-/-}$ (***N***, ***S***) piriform cortices. The LOT is outlined by a dashed white line, following the contours of the area of tight cellular packing. Quantitation of relative area measurements of the LOT in each genotype (***O***). Quantitation of the number of DAPI $^{+}$ cells displaced within the LOT (***T***). nc, Neocortex; pc, piriform cortex; str, striatum; tu, olfactory tubercle.

cious neurogenesis by limiting *Neurog2*'s ability to specify a CR cell fate. Hence, in the absence of *Neurog1*, more CR cells are generated. Furthermore, we reveal that *Neurog1* and *Neurog2* are required to specify the identity of a subset of CR neurons in the piriform cortex: lot guidepost cells. Accordingly, we demonstrate that *Trp73*, which is expressed in CR cells (Meyer et al., 2002, 2004) and lot cells (this study), is required for normal LOT axon innervation of the piriform cortex. Finally, we demonstrate that at later developmental stages, *Neurog1* and *Neurog2* change their fate specification properties in the ventral pallium, guiding the differentiation of layer II/III piriform cortical neurons.

Neurog1 and *Neurog2* have overlapping and nonoverlapping functions in CR progenitors

Neurog1 and Neurog2 are expressed in CR cell lineages derived from all three progenitor domains (this study; Dixit et al., 2011b), including the rostrobulbar area/pallial septum, cortical hem/choroid plexus, and ventral pallium (Takiguchi-Hayashi et al., 2004; Bielle et al., 2005; Yoshida et al., 2006; Zhao et al., 2006; García-Moreno et al., 2007; Imayoshi et al., 2008). *Neurog2*-derived CR cells are widespread, populating the piriform cortex, neocortex, and hippocampus (this study; Dixit et al., 2011b). It is thus not surprising that we observed a global reduction in CR cell numbers in all cortical domains in *Neurog1/2* $^{-/-}$ embryos. What was unexpected was the increase in CR numbers in *Neurog1* $^{-/-}$ embryos, and the ability of *Neurog1* to limit *Neurog2*'s ability to specify a Reelin $^{+}$ CR cell identity in gain-of-function assays. We suggest that the transition from generating CR neurons to deep-layer cortical neurons in the neocortex and piriform cortex depends on *Neurog1*'s ability to curtail *Neurog2*'s early proneural and cell fate specification properties. While future studies are required to address mechanism, it may be that Neurog1-Neurog2 heterodimers might have a reduced capacity to transactivate target genes compared with Neurog2-Neurog2 homodimers. In-

deed, in a previous study we revealed that *Neurog2*'s proneural activities are temporally regulated by their dimerization partner, and that Neurog2-Neurog2 homodimers are more active than Neurog2-E47 heterodimers (Li et al., 2012).

Unexpected was the striking and specific loss of *Trp73*$^{+}$ CR cells in a V-shaped wedge in the *Neurog1/2*$^{-/-}$ piriform cortex. *Trp73*$^{+}$ CR cells are thought to arise from the cortical hem and pallial septum (Meyer et al., 2002, 2004; Hanashima et al., 2007). However, in a *Dbx1*-lineage trace (Bielle et al., 2005), which labels CR cells derived from the ventral pallium and pallial septum, *lacZ*$^{+}$ cells accumulate in the piriform cortex in a pattern that closely resembles the wedge-shaped distribution of *Trp73*$^{+}$ cells (this study). While it has been suggested that pallial septum-derived CR cells in the *Dbx1* lineage are *Trp73*$^{+}$ (Griveau et al., 2010), our data support the idea that some of these *Trp73*$^{+}$ CR cells may also be derived from the ventral pallium. Interestingly, the pattern of *Trp73* expression in the wild-type piriform cortex is the same as lot1/*mGluR1*, which label lot guidepost cells (Sato et al., 1998; Hirata et al., 2012). Moreover, lot1/*mGluR1* expression was strikingly reduced in the *Neurog1/2*$^{-/-}$ piriform cortex. These data, combined with our coexpression data, are good evidence that lot guidepost cells are a subpopulation of CR cells that depend on *Neurog1* and *Neurog2* for their differentiation.

Neurog1 and *Neurog2* specify the identities of piriform cortical neurons

Recent studies have suggested that CR cells influence regional identities and boundary formation in the underlying cortical neuroepithelium (Griveau et al., 2010). Specifically, the loss of *Dbx1*, which is expressed in CR progenitors in the ventral pallium and pallial septum, alters the distribution of the remaining CR cells (Bielle et al., 2005), thereby shifting the regional borders that prefigure cortical areas (Griveau et al., 2010). Similar compensatory changes likely influence the distribution of remaining CR cells in *Neurog2*$^{-/-}$ and *Neurog1/2*$^{-/-}$ cortices. This raises the question of whether the patterning defects in *Neurog2*$^{-/-}$ and *Neurog1/2*$^{-/-}$ cortices are related in any way to CR cell changes. It is difficult to reach a definitive answer to this question, since the mis-specification of *Neurog2*$^{-/-}$ and *Neurog1/2*$^{-/-}$ cortical progenitors may instead be linked to a requirement to suppress expression of *Ascl1*, another proneural gene that specifies a ventral telencephalic phenotype (Fode et al., 2000; Schuurmans et al., 2004). Nevertheless, it is remarkable that the phenotype of the ectopic interneurons in *Neurog2*$^{-/-}$ and *Neurog1/2*$^{-/-}$ cortices most closely resemble OB interneurons (i.e., *Etv1*$^{+}$, Pax6^{+}, *Dlx1*$^{+}$, calretinin^{+}; Yun et al., 2001, 2003), an interneuron population that is normally derived from the dorsal LGE (Long et al., 2003, 2007; Stenman et al., 2003; Yun et al., 2003; Kohwi et al., 2005). Interestingly, the dorsal LGE is a subpallial progenitor domain that immediately abuts the ventral pallium (Yun et al., 2001). It is thus tempting to speculate that the mis-specification of *Neurog2*$^{-/-}$ and *Neurog1/2*$^{-/-}$ cortical territories may be due to a shift in the pallial–subpallial border, and that this shift may be related to alterations in the distribution and identity of CR cells. In contrast, the border between the neocortex and piriform cortex does not appear to be shifted in *Neurog1/2*$^{-/-}$ embryos, as the loss of piriform cortex markers does not correlate with an expansion of neocortical markers *Fezf1* and *Tle4*. In this regard, *Neurog1/2*$^{-/-}$ mutants differ from *Tbr1* mutants, which ectopically express neocortical markers in the piriform cortex (Hevner et al., 2001).

Based on marker expression (Hirata et al., 2002), as well as short-term lineage tracing using *Neurog2*$^{GFP\,KI}$ mice (this study) and long-term lineage tracing using *Dbx1-cre*^{KI} mice (Bielle et al., 2005), neurons in the piriform cortex are generated from progenitor cells in the ventral pallium. Hypocellularity of the *Neurog2*$^{-/-}$ and *Neurog1/2*$^{-/-}$ piriform cortices is likely related to increased apoptosis in the ventral pallium. Notably, in *Pax6* mutants, neuronal mis-specification leads to elevated apoptosis due to altered expression of the neurotrophin receptors TrkB and p75NTR (Nikoletopoulou et al., 2007). Interestingly, *Dbx1* expression, which marks the ventral pallium, is lost in *Pax6* mutants (Yun et al., 2001), whereas in *Neurog2*$^{-/-}$ and *Neurog1/2*$^{-/-}$ cortices, *Dbx1* expression is retained (this study). Moreover, *TrkB* expression persists in the *Neurog2*$^{-/-}$ and *Neurog1/2*$^{-/-}$ ventral pallium (data not shown), which undergoes massive cell death, suggesting that the expression of this neurotrophin receptor alone may not be sufficient to prevent apoptosis in mis-specified pallial progenitors.

CR cells function in axon guidance

The piriform cortex is part of the olfactory system, which also includes the OE and OB. While the OE, OB, and piriform cortex are separate functional entities, they develop as an interconnected unit (de Castro, 2009). Interestingly, *Neurog1* and/or *Neurog2* are expressed in progenitor cells for each of these components of the olfactory system, including the OE (Cau et al., 2002), OB (Winpenny et al., 2011; Shaker et al., 2012), and piriform cortex (this study). While the differentiation of olfactory sensory neurons is perturbed in *Neurog1*$^{-/-}$ single mutants, disruptions in OB (Shaker et al., 2012) and piriform cortex (this study) development are most severe in *Neurog1/2*$^{-/-}$ double mutants. *Neurog1/2*$^{-/-}$ embryos develop a hypocellular OBLS in an aberrant ventrolateral position (Shaker et al., 2012). However, even though some mitral cells differentiate in the *Neurog1/2*$^{-/-}$ OBLS (Shaker et al., 2012), we show here that these OB projection neurons fail to innervate the piriform cortex (i.e., form a LOT) due to the loss of lot guidepost cells (Sato et al., 1998). Notably, a similar OBLS phenotype is observed in *Pax6*$^{-/-}$ (Hirata et al., 2002), *Lhx2*$^{-/-}$ (Saha et al., 2007), and *Gli3*$^{-/-}$ (Balmer and LaMantia, 2004) mutants, yet only *Pax6*$^{-/-}$ mitral cells extend their axons out of the OB to form the LOT and innervate the piriform cortex (Hirata et al., 2002). In contrast, in *Gli3*$^{-/-}$ mutants, in which lot cells fail to migrate into the piriform cortex and instead accumulate in the neocortex (Tomioka et al., 2000; Balmer and LaMantia, 2004), and in *Lhx2*$^{-/-}$ cortices, where lot cells fail to differentiate (Saha et al., 2007), LOT formation is perturbed. CR cells thus have multiple roles in building the architecture of the cortex: not only in patterning the cortical VZ (Griveau et al., 2010), but also in axonal guidance of olfactory tracts (this study).

Through these findings, we provide new insights into the control of temporal identity transitions and neuronal fate specification in the piriform cortex, a poorly understood brain region. Moreover, we identify a novel population of CR neurons (lot cells), and ascribe a new function to *Trp73*, which is expressed in these lot/CR cells, in LOT formation.

References

Alam S, Zinyk D, Ma L, Schuurmans C (2005) Members of the Plag gene family are expressed in complementary and overlapping regions in the developing murine nervous system. Dev Dyn 234:772–782. CrossRef Medline

Alcántara S, Ruiz M, D'Arcangelo G, Ezan F, de Lecea L, Curran T, Sotelo C, Soriano E (1998) Regional and cellular patterns of reelin mRNA expression in the forebrain of the developing and adult mouse. J Neurosci 18:7779–7799. Medline

Anderson SA, Qiu M, Bulfone A, Eisenstat DD, Meneses J, Pedersen R, Rubenstein JL (1997) Mutations of the homeobox genes Dlx-1 and Dlx-2 disrupt the striatal subventricular zone and differentiation of late born striatal neurons. Neuron 19:27–37. CrossRef Medline

Assimacopoulos S, Grove EA, Ragsdale CW (2003) Identification of a Pax6-dependent epidermal growth factor family signaling source at the lateral edge of the embryonic cerebral cortex. J Neurosci 23:6399–6403. Medline

Backman M, Machon O, Mygland L, van den Bout CJ, Zhong W, Taketo MM, Krauss S (2005) Effects of canonical Wnt signaling on dorso-ventral specification of the mouse telencephalon. Dev Biol 279:155–168. CrossRef Medline

Balmer CW, LaMantia AS (2004) Loss of Gli3 and Shh function disrupts olfactory axon trajectories. J Comp Neurol 472:292–307. CrossRef Medline

Bielle F, Griveau A, Narboux-Nême N, Vigneau S, Sigrist M, Arber S, Wassef M, Pierani A (2005) Multiple origins of Cajal-Retzius cells at the borders of the developing pallium. Nat Neurosci 8:1002–1012. CrossRef Medline

Britz O, Mattar P, Nguyen L, Langevin LM, Zimmer C, Alam S, Guillemot F, Schuurmans C (2006) A role for proneural genes in the maturation of cortical progenitor cells. Cereb Cortex 16 [Suppl 1]:i138–i151. Medline

Cau E, Casarosa S, Guillemot F (2002) Mash1 and Ngn1 control distinct steps of determination and differentiation in the olfactory sensory neuron lineage. Development 129:1871–1880. Medline

Caviness VS Jr (1982) Neocortical histogenesis in normal and reeler mice: a developmental study based upon [3H]thymidine autoradiography. Brain Res 256:293–302. Medline

Chou SJ, Perez-Garcia CG, Kroll TT, O'Leary DD (2009) Lhx2 specifies regional fate in Emx1 lineage of telencephalic progenitors generating cerebral cortex. Nat Neurosci 12:1381–1389. CrossRef Medline

Conforti F, Sayan AE, Sreekumar R, Sayan BS (2012) Regulation of p73 activity by post-translational modifications. Cell Death Dis 3:e285. CrossRef Medline

D'Arcangelo G, Miao GG, Curran T (1996) Detection of the reelin breakpoint in reeler mice. Brain Res Mol Brain Res 39:234–236. CrossRef Medline

de Castro F (2009) Wiring olfaction: the cellular and molecular mechanisms that guide the development of synaptic connections from the nose to the cortex. Front Neurosci 3:52. CrossRef Medline

de Carlos JA, López-Mascaraque L, Valverde F (1996) Dynamics of cell migration from the lateral ganglionic eminence in the rat. J Neurosci 16:6146–6156. Medline

Dixit R, Lu F, Cantrup R, Gruenig N, Langevin LM, Kurrasch DM, Schuurmans C (2011a) Efficient gene delivery into multiple CNS territories using *in utero* electroporation. J Vis Exp pii:2957. CrossRef Medline

Dixit R, Zimmer C, Waclaw RR, Mattar P, Shaker T, Kovach C, Logan C, Campbell K, Guillemot F, Schuurmans C (2011b) Ascl1 participates in Cajal-Retzius cell development in the neocortex. Cereb Cortex 21:2599–2611. CrossRef Medline

Flames N, Hobert O (2009) Gene regulatory logic of dopamine neuron differentiation. Nature 458:885–889. CrossRef Medline

Fode C, Gradwohl G, Morin X, Dierich A, LeMeur M, Goridis C, Guillemot F (1998) The bHLH protein NEUROGENIN 2 is a determination factor for epibranchial placode-derived sensory neurons. Neuron 20:483–494. CrossRef Medline

Fode C, Ma Q, Casarosa S, Ang SL, Anderson DJ, Guillemot F (2000) A role for neural determination genes in specifying the dorsoventral identity of telencephalic neurons. Genes Dev 14:67–80. Medline

Fujitani M, Cancino GI, Dugani CB, Weaver IC, Gauthier-Fisher A, Paquin A, Mak TW, Wojtowicz MJ, Miller FD, Kaplan DR (2010) TAp73 acts via the bHLH Hey2 to promote long-term maintenance of neural precursors. Curr Biol 20:2058–2065. CrossRef Medline

García-Moreno F, López-Mascaraque L, De Carlos JA (2007) Origins and migratory routes of murine Cajal-Retzius cells. J Comp Neurol 500:419–432. CrossRef Medline

Gorski JA, Talley T, Qiu M, Puelles L, Rubenstein JL, Jones KR (2002) Cortical excitatory neurons and glia, but not GABAergic neurons, are produced in the Emx1-expressing lineage. J Neurosci 22:6309–6314. Medline

Griveau A, Borello U, Causeret F, Tissir F, Boggetto N, Karaz S, Pierani A (2010) A novel role for Dbx1-derived Cajal-Retzius cells in early regionalization of the cerebral cortical neuroepithelium. PLoS Biol 8:e1000440. CrossRef Medline

Gunhaga L, Marklund M, Sjödal M, Hsieh JC, Jessell TM, Edlund T (2003) Specification of dorsal telencephalic character by sequential Wnt and FGF signaling. Nat Neurosci 6:701–707. CrossRef Medline

Hanashima C, Fernandes M, Hebert JM, Fishell G (2007) The role of Foxg1 and dorsal midline signaling in the generation of Cajal-Retzius subtypes. J Neurosci 27:11103–11111. CrossRef Medline

Hevner RF, Shi L, Justice N, Hsueh Y, Sheng M, Smiga S, Bulfone A, Goffinet AM, Campagnoni AT, Rubenstein JL (2001) Tbr1 regulates differentiation of the preplate and layer 6. Neuron 29:353–366. CrossRef Medline

Hevner RF, Neogi T, Englund C, Daza RA, Fink A (2003) Cajal-Retzius cells in the mouse: transcription factors, neurotransmitters, and birthdays suggest a pallial origin. Brain Res Dev Brain Res 141:39–53. CrossRef Medline

Hirabayashi Y, Itoh Y, Tabata H, Nakajima K, Akiyama T, Masuyama N, Gotoh Y (2004) The Wnt/beta-catenin pathway directs neuronal differentiation of cortical neural precursor cells. Development 131:2791–2801. CrossRef Medline

Hirata T, Nomura T, Takagi Y, Sato Y, Tomioka N, Fujisawa H, Osumi N (2002) Mosaic development of the olfactory cortex with Pax6-dependent and -independent components. Brain Res Dev Brain Res 136:17–26. CrossRef Medline

Hirata T, Kumada T, Kawasaki T, Furukawa T, Aiba A, Conquet F, Saga Y, Fukuda A (2012) Guidepost neurons for the lateral olfactory tract: expression of metabotropic glutamate receptor 1 and innervation by glutamatergic olfactory bulb axons. Dev Neurobiol 72:1559–1576. CrossRef Medline

Howell BW, Hawkes R, Soriano P, Cooper JA (1997) Neuronal position in the developing brain is regulated by mouse disabled-1. Nature 389:733–737. CrossRef Medline

Imayoshi I, Shimogori T, Ohtsuka T, Kageyama R (2008) Hes genes and neurogenin regulate nonneural versus neural fate specification in the dorsal telencephalic midline. Development 135:2531–2541. CrossRef Medline

Israsena N, Hu M, Fu W, Kan L, Kessler JA (2004) The presence of FGF2 signaling determines whether beta-catenin exerts effects on proliferation or neuronal differentiation of neural stem cells. Dev Biol 268:220–231. CrossRef Medline

Kohwi M, Osumi N, Rubenstein JL, Alvarez-Buylla A (2005) Pax6 is required for making specific subpopulations of granule and periglomerular neurons in the olfactory bulb. J Neurosci 25:6997–7003. CrossRef Medline

Li S, Mattar P, Zinyk D, Singh K, Chaturvedi CP, Kovach C, Dixit R, Kurrasch DM, Ma YC, Chan JA, Wallace V, Dilworth FJ, Brand M, Schuurmans C (2012) GSK3 temporally regulates neurogenin 2 proneural activity in the neocortex. J Neurosci 32:7791–7805. CrossRef Medline

Long JE, Garel S, Depew MJ, Tobet S, Rubenstein JL (2003) DLX5 regulates development of peripheral and central components of the olfactory system. J Neurosci 23:568–578. Medline

Long JE, Garel S, Alvarez-Dolado M, Yoshikawa K, Osumi N, Alvarez-Buylla A, Rubenstein JL (2007) Dlx-dependent and -independent regulation of olfactory bulb interneuron differentiation. J Neurosci 27:3230–3243. CrossRef Medline

Ma Q, Chen Z, del Barco Barrantes I, de la Pompa JL, Anderson DJ (1998) Neurogenin1 is essential for the determination of neuronal precursors for proximal cranial sensory ganglia. Neuron 20:469–482. CrossRef Medline

Machon O, Backman M, Krauss S, Kozmik Z (2005) The cellular fate of cortical progenitors is not maintained in neurosphere cultures. Mol Cell Neurosci 30:388–397. CrossRef Medline

Marín-Padilla M (1998) Cajal-Retzius cells and the development of the neocortex. Trends Neurosci 21:64–71. CrossRef Medline

Mattar P, Britz O, Johannes C, Nieto M, Ma L, Rebeyka A, Klenin N, Polleux F, Guillemot F, Schuurmans C (2004) A screen for downstream effectors of Neurogenin2 in the embryonic neocortex. Dev Biol 273:373–389. CrossRef Medline

Mattar P, Langevin LM, Markham K, Klenin N, Shivji S, Zinyk D, Schuurmans C (2008) Basic helix-loop-helix transcription factors cooperate to specify a cortical projection neuron identity. Mol Cell Biol 28:1456–1469. CrossRef Medline

Meyer G, Perez-Garcia CG, Abraham H, Caput D (2002) Expression of p73 and Reelin in the developing human cortex. J Neurosci 22:4973–4986. Medline

Meyer G, Cabrera Socorro A, Perez Garcia CG, Martinez Millan L, Walker N,

Caput D (2004) Developmental roles of p73 in Cajal-Retzius cells and cortical patterning. J Neurosci 24:9878–9887. CrossRef Medline

Mohamed OA, Clarke HJ, Dufort D (2004) Beta-catenin signaling marks the prospective site of primitive streak formation in the mouse embryo. Dev Dyn 231:416–424. CrossRef Medline

Nikoletopoulou V, Plachta N, Allen ND, Pinto L, Götz M, Barde YA (2007) Neurotrophin receptor-mediated death of misspecified neurons generated from embryonic stem cells lacking Pax6. Cell Stem Cell 1:529–540. CrossRef Medline

O'Dell RS, Ustine CJ, Cameron DA, Lawless SM, Williams RM, Zipfel WR, Olson EC (2012) Layer 6 cortical neurons require Reelin-Dab1 signaling for cellular orientation, Golgi deployment, and directed neurite growth into the marginal zone. Neural Dev 7:25. CrossRef Medline

Pearson BJ, Doe CQ (2004) Specification of temporal identity in the developing nervous system. Annu Rev Cell Dev Biol 20:619–647. CrossRef Medline

Puelles L, Kuwana E, Puelles E, Bulfone A, Shimamura K, Keleher J, Smiga S, Rubenstein JL (2000) Pallial and subpallial derivatives in the embryonic chick and mouse telencephalon, traced by the expression of the genes Dlx-2, Emx-1, Nkx-2.1, Pax-6, and Tbr-1. J Comp Neurol 424:409–438. CrossRef Medline

Saha B, Hari P, Huilgol D, Tole S (2007) Dual role for LIM-homeodomain gene Lhx2 in the formation of the lateral olfactory tract. J Neurosci 27:2290–2297. CrossRef Medline

Saino-Saito S, Cave JW, Akiba Y, Sasaki H, Goto K, Kobayashi K, Berlin R, Baker H (2007) ER81 and CaMKIV identify anatomically and phenotypically defined subsets of mouse olfactory bulb interneurons. J Comp Neurol 502:485–496. CrossRef Medline

Sakamoto M, Hirata H, Ohtsuka T, Bessho Y, Kageyama R (2003) The basic helix-loop-helix genes Hesr1/Hey1 and Hesr2/Hey2 regulate maintenance of neural precursor cells in the brain. J Biol Chem 278:44808–44815. CrossRef Medline

Sarma AA, Richard MB, Greer CA (2011) Developmental dynamics of piriform cortex. Cereb Cortex 21:1231–1245. CrossRef Medline

Sato Y, Hirata T, Ogawa M, Fujisawa H (1998) Requirement for early-generated neurons recognized by monoclonal antibody lot1 in the formation of lateral olfactory tract. J Neurosci 18:7800–7810. Medline

Schuurmans C, Armant O, Nieto M, Stenman JM, Britz O, Klenin N, Brown C, Langevin LM, Seibt J, Tang H, Cunningham JM, Dyck R, Walsh C, Campbell K, Polleux F, Guillemot F (2004) Sequential phases of cortical specification involve Neurogenin-dependent and -independent pathways. EMBO J 23:2892–2902. CrossRef Medline

Shaker T, Dennis D, Kurrasch DM, Schuurmans C (2012) Neurog1 and Neurog2 coordinately regulate development of the olfactory system. Neural Dev 7:28. CrossRef Medline

Smart IH, Smart M (1977) The location of nuclei of different labelling intensities in autoradiographs of the anterior forebrain of postnatial mice injected with [3H]thymidine on the eleventh and twelfth days postconception. J Anat 123:515–525. Medline

Stenman J, Toresson H, Campbell K (2003) Identification of two distinct progenitor populations in the lateral ganglionic eminence: implications for striatal and olfactory bulb neurogenesis. J Neurosci 23:167–174. Medline

Supèr H, Soriano E, Uylings HB (1998) The functions of the preplate in development and evolution of the neocortex and hippocampus. Brain Res Brain Res Rev 27:40–64. CrossRef Medline

Takahashi T, Goto T, Miyama S, Nowakowski RS, Caviness VS Jr (1999) Sequence of neuron origin and neocortical laminar fate: relation to cell cycle of origin in the developing murine cerebral wall. J Neurosci 19:10357–10371. Medline

Takiguchi-Hayashi K, Sekiguchi M, Ashigaki S, Takamatsu M, Hasegawa H, Suzuki-Migishima R, Yokoyama M, Nakanishi S, Tanabe Y (2004) Generation of reelin-positive marginal zone cells from the caudomedial wall of telencephalic vesicles. J Neurosci 24:2286–2295. CrossRef Medline

Tomioka N, Osumi N, Sato Y, Inoue T, Nakamura S, Fujisawa H, Hirata T (2000) Neocortical origin and tangential migration of guidepost neurons in the lateral olfactory tract. J Neurosci 20:5802–5812. Medline

Vergaño-Vera E, Yusta-Boyo MJ, de Castro F, Bernad A, de Pablo F, Vicario-Abejón C (2006) Generation of GABAergic and dopaminergic interneurons from endogenous embryonic olfactory bulb precursor cells. Development 133:4367–4379. CrossRef Medline

Vyas A, Saha B, Lai E, Tole S (2003) Paleocortex is specified in mice in which dorsal telencephalic patterning is severely disrupted. J Comp Neurol 466:545–553. CrossRef Medline

Wang Z, Shu W, Lu MM, Morrisey EE (2005) Wnt7b activates canonical signaling in epithelial and vascular smooth muscle cells through interactions with Fzd1, Fzd10, and LRP5. Mol Cell Biol 25:5022–5030. CrossRef Medline

Watanabe K, Kamiya D, Nishiyama A, Katayama T, Nozaki S, Kawasaki H, Watanabe Y, Mizuseki K, Sasai Y (2005) Directed differentiation of telencephalic precursors from embryonic stem cells. Nat Neurosci 8:288–296. CrossRef Medline

Winpenny E, Lebel-Potter M, Fernandez ME, Brill MS, Götz M, Guillemot F, Raineteau O (2011) Sequential generation of olfactory bulb glutamatergic neurons by Neurog2-expressing precursor cells. Neural Dev 6:12. CrossRef Medline

Wood JG, Martin S, Price DJ (1992) Evidence that the earliest generated cells of the murine cerebral cortex form a transient population in the subplate and marginal zone. Brain Res Dev Brain Res 66:137–140. CrossRef Medline

Yoshida M, Assimacopoulos S, Jones KR, Grove EA (2006) Massive loss of Cajal-Retzius cells does not disrupt neocortical layer order. Development 133:537–545. CrossRef Medline

Yun K, Potter S, Rubenstein JL (2001) Gsh2 and Pax6 play complementary roles in dorsoventral patterning of the mammalian telencephalon. Development 128:193–205. Medline

Yun K, Garel S, Fischman S, Rubenstein JL (2003) Patterning of the lateral ganglionic eminence by the Gsh1 and Gsh2 homeobox genes regulates striatal and olfactory bulb histogenesis and the growth of axons through the basal ganglia. J Comp Neurol 461:151–165. CrossRef Medline

Zhao C, Guan W, Pleasure SJ (2006) A transgenic marker mouse line labels Cajal-Retzius cells from the cortical hem and thalamocortical axons. Brain Res 1077:48–53. CrossRef Medline

Zimmer C, Lee J, Griveau A, Arber S, Pierani A, Garel S, Guillemot F (2010) Role of Fgf8 signalling in the specification of rostral Cajal-Retzius cells. Development 137:293–302. CrossRef Medline